Access to Monomeric Hydridoplumbate(II) Anions with Remarkable Thermostability

Shuo Wang, Han-Jung Li, Wan-Ching Lee, Shuo-Ling Huang, Wen Chun Wu, Fong-Ku Shi Ting-Shen Kuo, I-Chung Lu, and Hsueh-Ju Liu*

1. Experimental details, synthetic procedures, and characterizations

All manipulations with oxygen and moisture sensitive materials were performed in a nitrogen-filled glovebox Solvents were dried and deaerated using a solvent system (AsiaWong Enterprise co., Ltd.) prior to use. Benzene-d_6 and tetrahydrofuran-d_8 (THF-d_8) was dried over sodium and benzophenone, degassed by three freeze-pump-thaw cycles, and stored under nitrogen over 3 Å molecular sieves. KB^sBu_3H (K-selectride) was purchased from Sigma-Aldrich, used as received and stored in freezer of a glovebox. Cryptand-222 and 18-crown-6 were purchased from Sigma-Aldrich, used as received and stored in a glovebox. The compounds **H_2L**,[1] $Pb(HMDS)_2$[2] and DBpin[3] were prepared according to literature procedures. The NMR spectra were recorded using Bruker 300, Varian 400 or Varian 600 MHz spectrometers. The NMR spectra were referenced to residual protonated solvent for ^1H NMR (3.58 ppm for compound in THF-d_8; 7.16 ppm for compound in benzene-d_6), to deuterated solvent for ^{13}C NMR (67.21 ppm for compound in THF-d_8 and 128.06 for compound in benzene-d_6), and to $Pb(NO)_3$ for ^{207}Pb NMR (0 ppm in D_2O). All spectra were recorded at 25 °C. Complex multiplets are noted as “m” and broad resonances as “br”. Elemental analyses were performed using an Elementar vario EL CUBE (CHN-OS Rapid, German). IR spectra were recorded in a glovebox and measured with Thermo Scientific NicoletTM Summit Fourier transform infrared (FT-IR) spectrometer with an attenuated-total-reflectance (ATR) attachment. The transmittance band positions are reported uncorrected, in reciprocal centimeters.

1.1 Synthesis of all compounds.

Synthesis of LPbTHF$_2$ (1-THF$_2$).

A solution of Pb(HMDS)$_2$ (719.5 mg, 1.36 mmol) in 5 mL of toluene was added to a solution of **H$_2$L** (699.9 mg, 1.36 mmol) in 10 mL of toluene at ambient temperature. The solution turned to red from yellow immediately and resulted in visible precipitates. After stirring at ambient temperature for 13 h, the mixture was cooled to –35 °C, and the supernatant was removed by decanting. The remaining solid was washed three times with 10 mL of pentane and then dried under vacuum to afford a red-orange powder **{LPb}$_n$**. Yield: 930.5 mg (95%). This product is barely soluble in benzene or toluene, whereas it reacts with THF to form the monomeric adduct **1-THF$_2$** that is soluble in THF. Red-orange crystals were obtained by diffusion of pentane into the saturated THF solution at –35 °C for 5 days. Yield: 85%.**^{1}H NMR** (500 MHz, THF-d_8) δ = 7.62 (d, *J* = 7.3Hz, 4H), 7.38 (d, *J* = 7.0 Hz, 4H), 7.30–7.23 (m, 8H), 7.16 (t, *J* = 7.4 Hz, 2H), 7.10 (t, J = 7.9 Hz, 1H), 7.05 (t, *J* = 7.4Hz, 2H), 6.90 (d, *J* = 7.9Hz, 2H), 6.52 (s, 2H) ppm; **^{13}C{^{1}H} NMR** (151 MHz, THF-d_8) δ = 155.58, 144.78, 140.41, 138.72, 137.93, 130.90, 130.05, 129.24, 128.84, 128.69, 126.22, 125.65, 125.45, 115.72, 114.03 ppm; **^{207}Pb{^{1}H} NMR** (105 MHz, THF-d_8) δ = 422.8 ppm. Anal. calcd for $C_{49}H_{49}N_3O_3Pb$ (**1-THF$_2$·THF**): C, 62.94; H, 5.28; N, 4.49. Found: C, 63.33; H, 5.29; N, 4.48.

Synthesis of [K18c6][1-H].

A solution of k-selectride (48.6 µL, 0.049 mmol) in 1.5 mL THF was cooled at –35°C and was added dropwise to a precooled solution containing **{LPb}$_n$** (35.2 mg, 0.049 mmol) and excess 18-crown-6 (32.1 mg, 0.121 mmol) in 5 mL THF. The clear orange red solution turned yellow was observed upon addition. The mixture was warmed to ambient temperature and stirred for 10 minutes, and was concentrated under vacuum to ca. 2 mL. Addition of pentane resulted in the formation of a yellow powder, and the supernatant was removed by decanting. The remaining solid was washed three times with 5 mL of pentane and then dried under vacuum to afford a yellow powder. Yield: 45.5 mg (81%). **^{1}H NMR** (600 MHz, THF-d_8, 263K): δ = 41.40 (s, $^{1}J_{^{207}\mathrm{PbH}}$ = 1312 Hz, 1H, PbH), 7.76 (d, *J* = 7.6 Hz, 4H), 7.40 (d, *J* = 7.2 Hz, 4H), 7.22 (q, *J* = 7.4 Hz, 8H), 7.08 (t, *J* = 7.4 Hz, 2H), 6.94 (t, *J* = 7.2 Hz, 2H), 6.84 (q, *J* = 5.4 Hz, 3H), 6.46 (s, 2H), 3.32 (s, 36H, O–$\underline{CH_2}$–$\underline{CH_2}$–O of 18-crown-6) ppm. **^{13}C{^{1}H} NMR** (151 MHz, THF-d_8, 263K): δ = 156.61, 142.97, 142.56, 140.50, 136.63, 135.45, 130.14, 128.67, 128.35, 128.24, 125.29, 124.89, 123.96, 114.36, 112.96, 71.00 ppm. **^{207}Pb{^{1}H} NMR** (104.84 MHz, THF-d_8, 263K): δ = 1450.1 (d, $^{1}J_{^{207}\mathrm{PbH}}$ = 1320 Hz) ppm.

Synthesis of [Kcrypt222][1-H].

A solution of k-selectride (208.9 µL, 0.209 mmol) in 1.5 mL THF was cooled at –35 °C and was added dropwise to a precooled solution containing **{LPb}$_n$** (150.2 mg, 0.209 mmol) and [2.2.2]-cryptand (78.6 mg, 0.209 mmol) in 10 mL THF. The clear orange red solution turned yellow was observed upon addition. The mixture was warmed to ambient temperature and stirred for 10 minutes, and the volume of the solution was concentrated under vacuum to ca. 2 mL. Diffusion of pentane into the filtered and saturated THF solution at –35 °C afforded yellow crystals of **[Kcrypt222][1-H]**. Yield: 213.5 mg (90%). Due to the low solubility of **[Kcrypt222][1-H]** in THF-d_8 (<1-2 mg/mL), no satisfactory ^{13}C and ^{207}Pb resonances were found after prolonged scans. **^{1}H NMR** (600 MHz, THF-d_8, 263K): δ = 41.66 (s, 1H, Pb*H*), 7.82 (d, *J* = 7.6 Hz, 4H), 7.44 (d, *J* = 7.2 Hz, 4H), 7.29 – 7.21 (m, 8H), 7.11 (t, *J* = 7.5 Hz, 2H), 6.97 (t, *J* = 7.3 Hz, 2H), 6.93 – 6.85 (m, 3H), 6.51 (s, 2H), 3.33 (s, 12H, O–$\underline{CH_2}$–$\underline{CH_2}$–O), 3.30 – 3.23 (m, 12H, O–$\underline{CH_2}$–CH$_2$–N), 2.33 – 2.29 (m, 12H, N–$\underline{CH_2}$–CH$_2$–O) ppm. Anal. calcd for $C_{55}H_{62}KN_5O_6Pb$: C, 58.18; H, 5.50 ; N, 6.17. Found: C, 58.56; H, 5.35; N, 6.17. ESI-MS calcd for $[C_{37}H_{26}N_3Pb]^-$: 720.19. Found: 720.33.

Synthesis of [Kcrypt222][1-OBz] and [K18c6][1-OBz].

Method 1: Benzaldehyde (3.8 mg, 0.036 mmol) was added to a precooled solution of **[Kcrypt222][1-H]** (40.6 mg, 0.036 mmol) in 10 mL THF at –35 °C, and the resulting solution was stirred at ambient temperature for 1 hr. The cloudy yellow solution turned into a clear orange-yellow solution was observed immediately. The solution was filtered through a plug of Celite, and the filtrate was dried under vacuum. Yield: 40.22 mg (90%). Cooling down the hot, saturated benzene solution of **[Kcrypt222][1-OBz]** afforded analytically pure yellow crystals.

Method 2: A precooled solution of potassium benzyloxide (4.12 mg, 0.028 mmol) in 2 mL THF was added to a THF solution containing **$\{LPb\}_n$** (20.3 mg, 0.028 mmol), and [2.2.2]-cryptand (10.8 mg, 0.029 mmol) at –35°C. The resulting solution turned orange yellow was observed and stirred at room temperature for 2 hrs. The solution was filtered through a plug of Celite, and the filtrate was dried under vacuum. Yield: 29.8 mg (85%).

^{1}H NMR (400 MHz, THF-d_8) δ = 8.12 (d, *J* = 7.7 Hz, 4H), 7.44 (d, *J* = 7.6 Hz, 4H), 7.24 (q, *J* = 7.2, 6.7 Hz, 10H), 7.12 (t, *J* = 7.3 Hz, 2H), 6.97 (q, *J* = 7.6 Hz, 4H), 6.90 (t, *J* = 5.1 Hz, 3H), 6.84 (t, *J* = 7.1 Hz, 1H), 6.51 (s, 2H), 5.37 (s, 2H), 3.21 (s, 12H, O–$\underline{CH_2}$–$\underline{CH_2}$–O), 3.14 (t, *J* = 4.17 Hz, 12H, O–$\underline{CH_2}$–CH_2–N), 2.18 (t, *J* = 4.17 Hz, 12H, N–$\underline{CH_2}$–CH_2–O) ppm. **^{13}C{^{1}H} NMR** (101 MHz, THF-d_8) δ = 156.13, 152.65, 144.01, 142.12, 140.11, 136.79, 136.32, 130.13, 129.92, 128.72, 128.36, 127.43, 127.03, 126.46, 125.36, 124.67, 124.13, 114.91, 112.89, 70.90, 69.07, 68.00, 54.29 ppm. **^{207}Pb{^{1}H} NMR** (126 MHz, THF-d_8) δ = 874.6 ppm. Anal. calcd for **Kcrypt222][1-OBz]**·0.5 benzene ($C_{65}H_{71}KN_5O_7Pb$): C, 60.96; H, 5.59; N, 5.47. Found: C, 60.98; H, 5.61; N, 5.74.

[K18c6][1-OBz] can be obtained in a similar procedure with yield of 26.1 mg (82%).

Synthesis of [K18c6][1-D].

To a precooled solution of **[K18c6][1-OBz]** (19.8 mg, 0.017 mmol) in THF, deuterated pinacolborane (DBpin, 0.138 M in C_6D_6, 127 µL, 0.017 mmol) was added, and the mixture was stirred at room temperature for 10 mins. The solution was then concentrated under vacuum to ca. 2 mL. Addition of pentane resulted in the formation of a yellow powder, and the supernatant was removed by decanting. The remaining solid was washed three times with 5 mL of pentane and then dried under vacuum to afford a yellow powder **[K18c6][1-D]**. Yield: 45.5 mg (81%). **[K1crypt222][1-D]** can be obtained in a similar manner with yield of 36.8 mg (94%).

^{1}H NMR (400 MHz, THF-d_8) δ = 7.77 (d, *J* = 7.4 Hz, 4H), 7.43 (d, *J* = 7.3 Hz, 4H), 7.32 – 7.21 (m, 8H), 7.12 (t, *J* = 7.3 Hz, 2H), 6.98 (t, *J* = 7.1 Hz, 2H), 6.89 (m, 3H), 6.49 (s, 2H), 3.32 (s, 36H, 18-crown-6) ppm. **^{2}H NMR** (61 MHz, THF-d_8) δ = 40.93 (s, 1H) ppm. **^{207}Pb NMR** (126 MHz, THF-d_8) δ = 1445.1 (br) ppm. ESI-MS calcd for $[C_{37}H_{25}DN_3Pb]^-$: 721.20. Found: 721.42.

1.2 NMR spectra of all compounds.

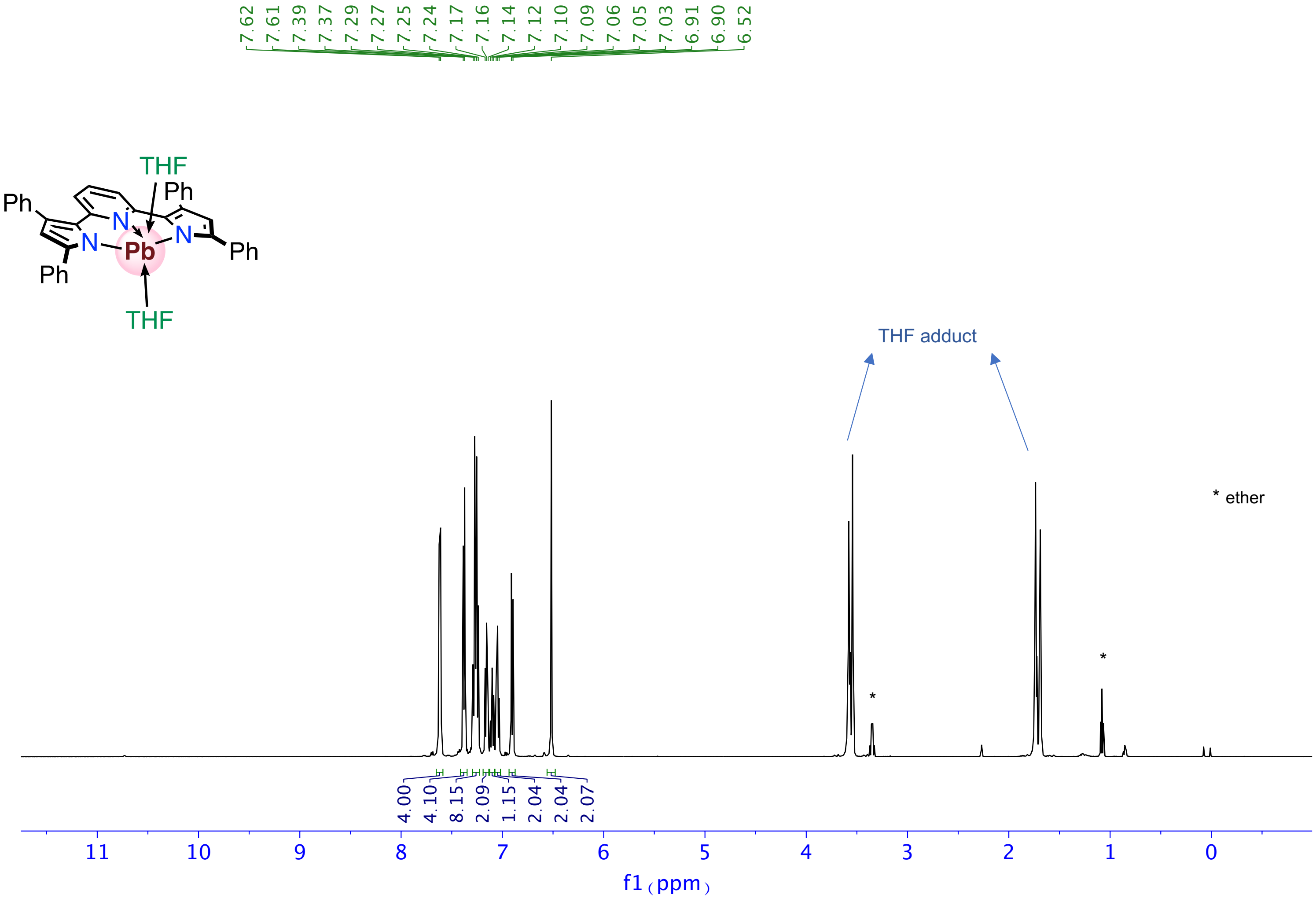

Figure S1. ^{1}H NMR spectrum of **1-THF$_2$** (THF-d_8, 298K)

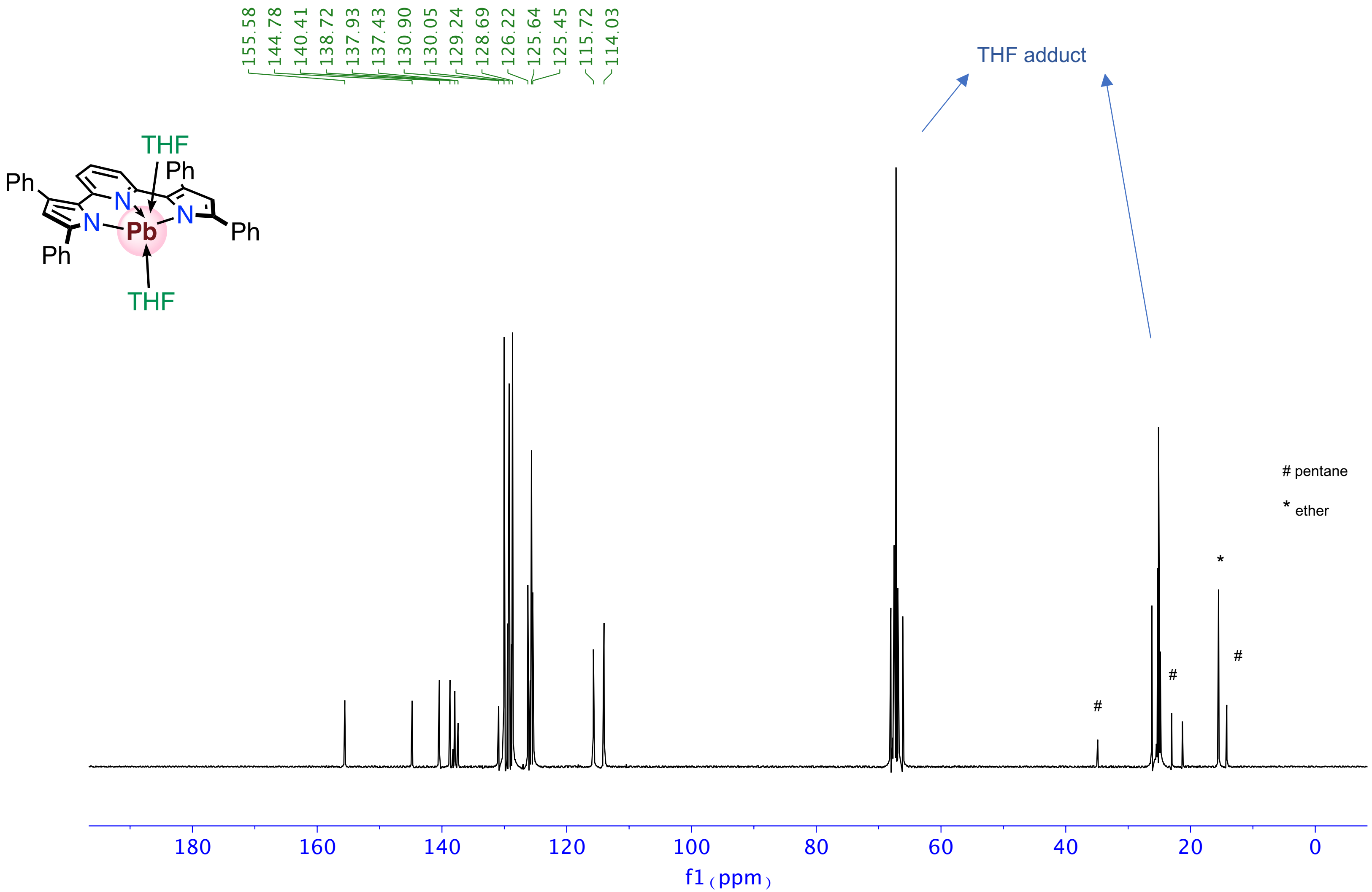

Figure S2. $^{13}C\{^1H\}$ NMR spectrum of **1-THF₂** (THF-*d*₈, 298K)

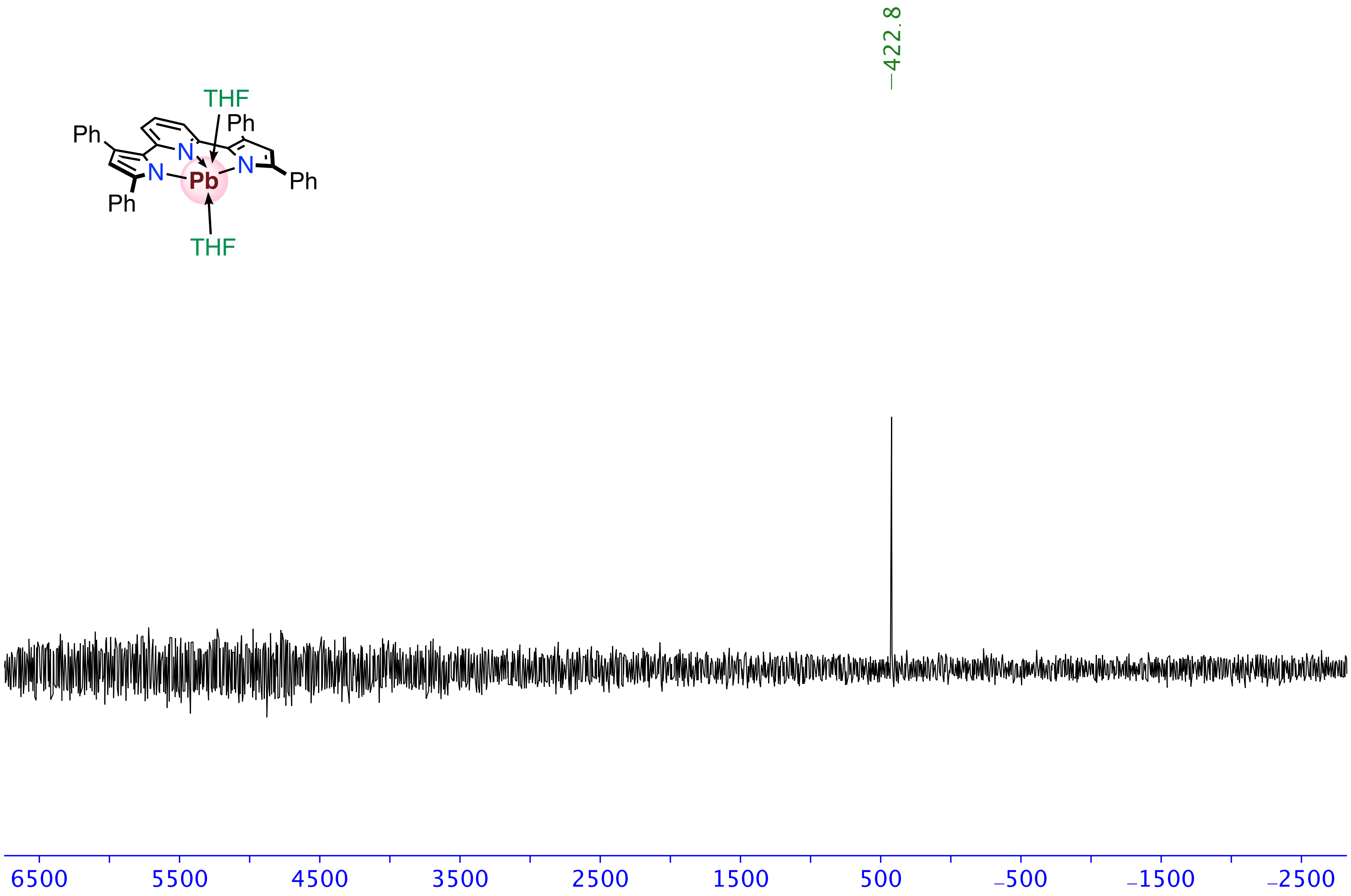

Figure S3. ^{207}Pb{^{1}H} NMR spectrum of **1-THF$_2$** (THF-d_8, 298K)

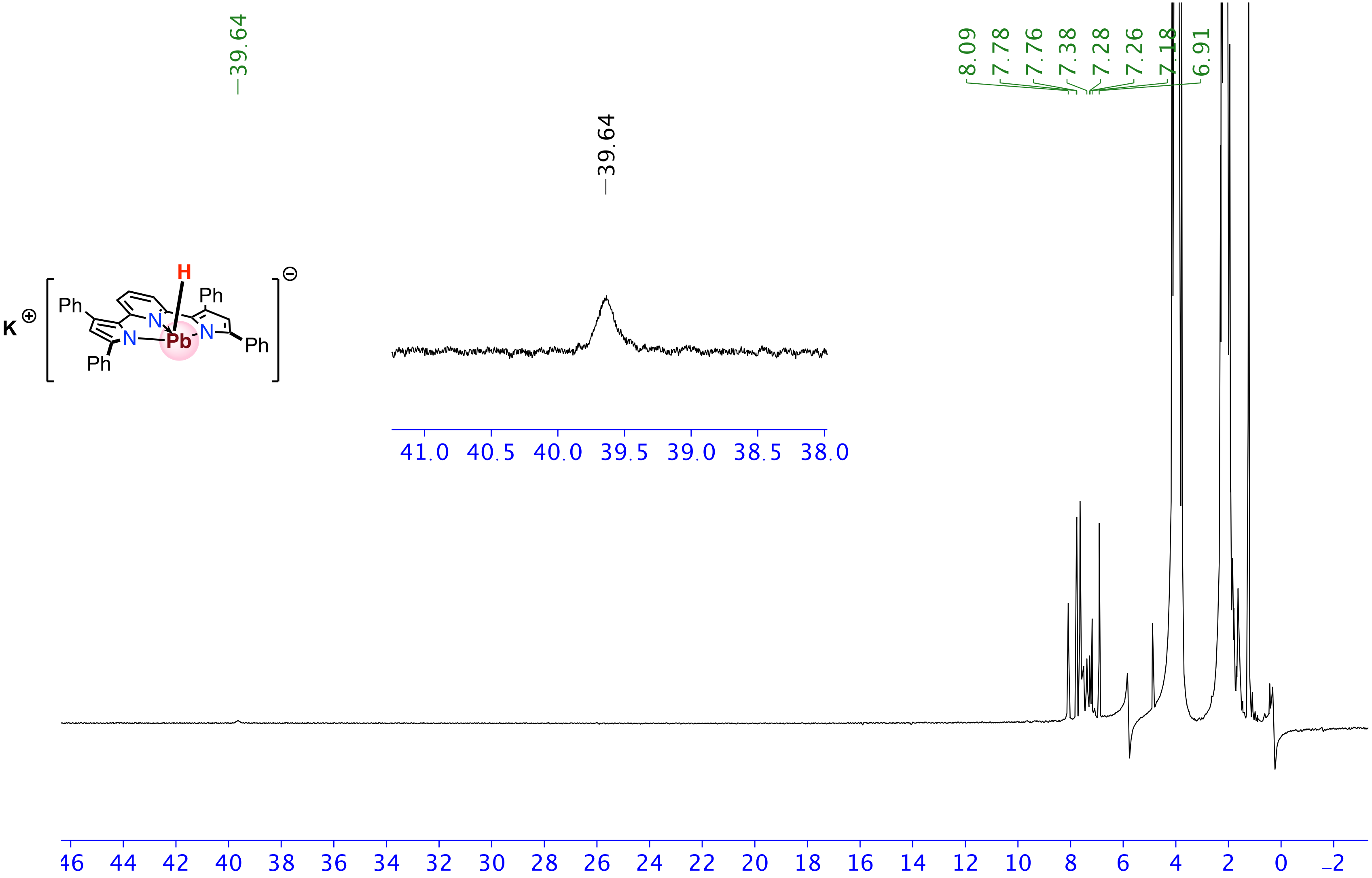

Figure S4. ^{1}H NMR spectrum of **K$^+$[1-H]** (THF/C$_6$D$_6$ capillary, 263K)

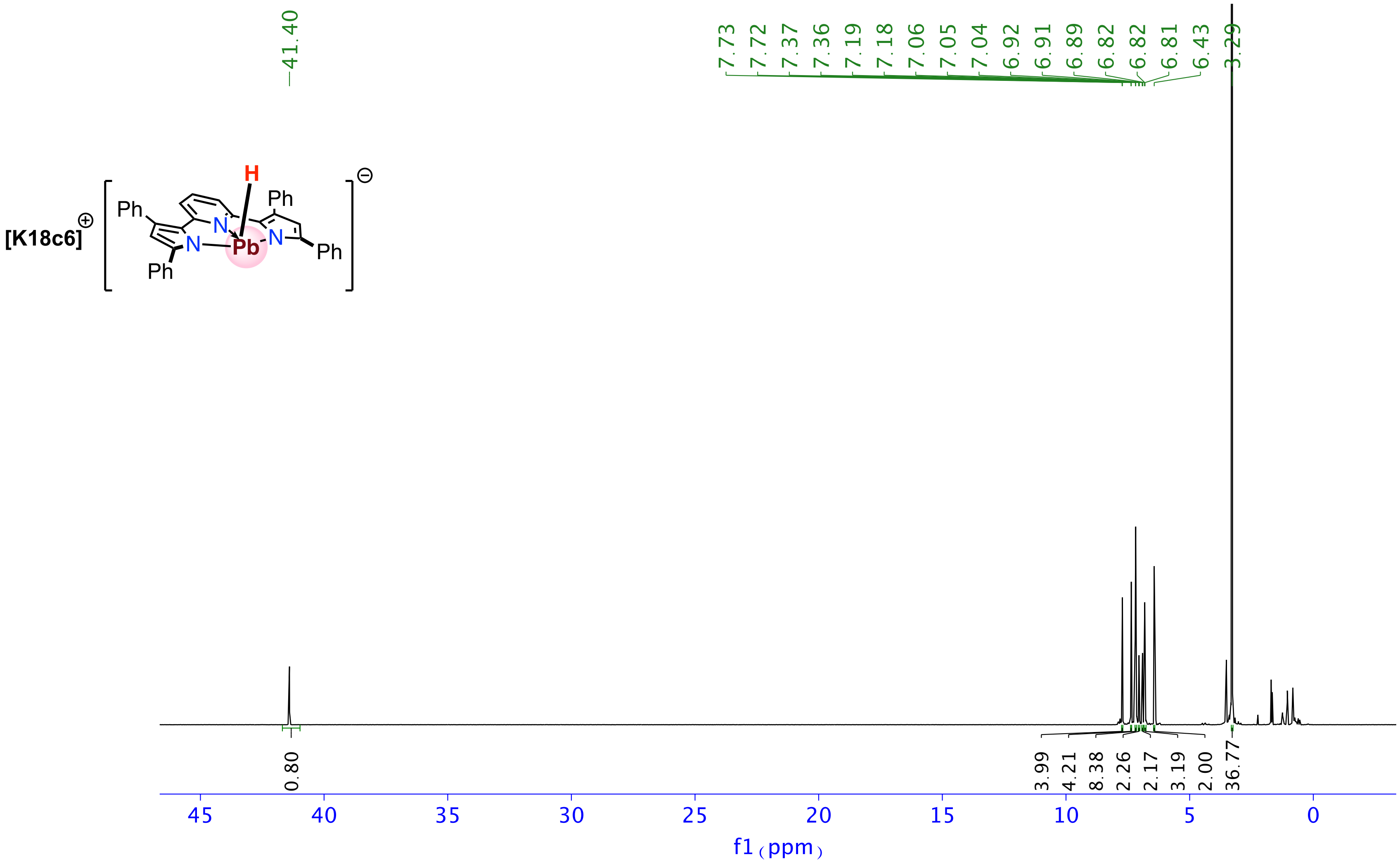

Figure S5. ^{1}H NMR spectrum of **[K18c6][1-H]** (THF-d_8, 263K)

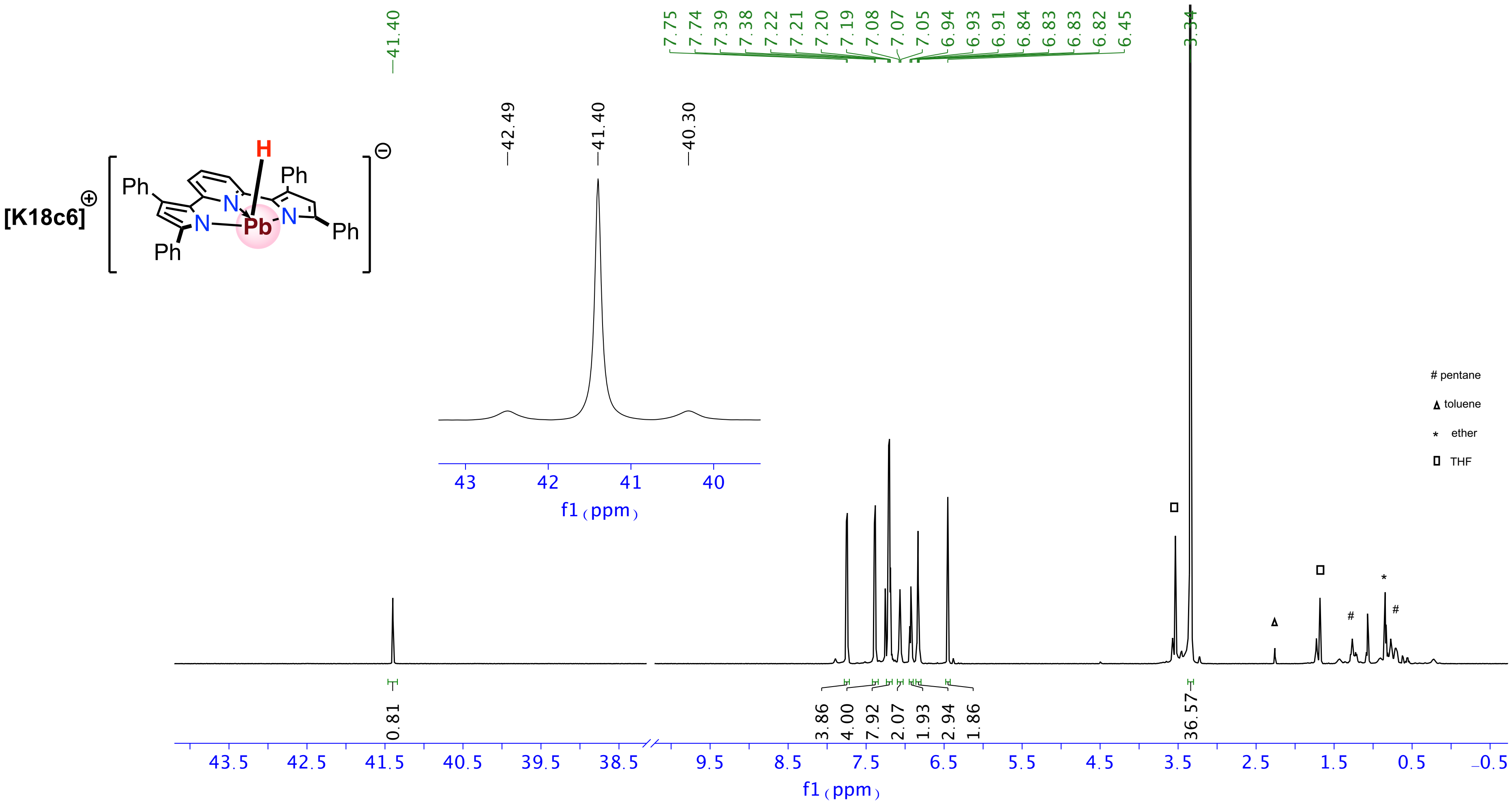

Figure S6. The enlarged part of the ^{1}H NMR spectrum of **[K18c6][1-H]** (THF-d_8, 263K)

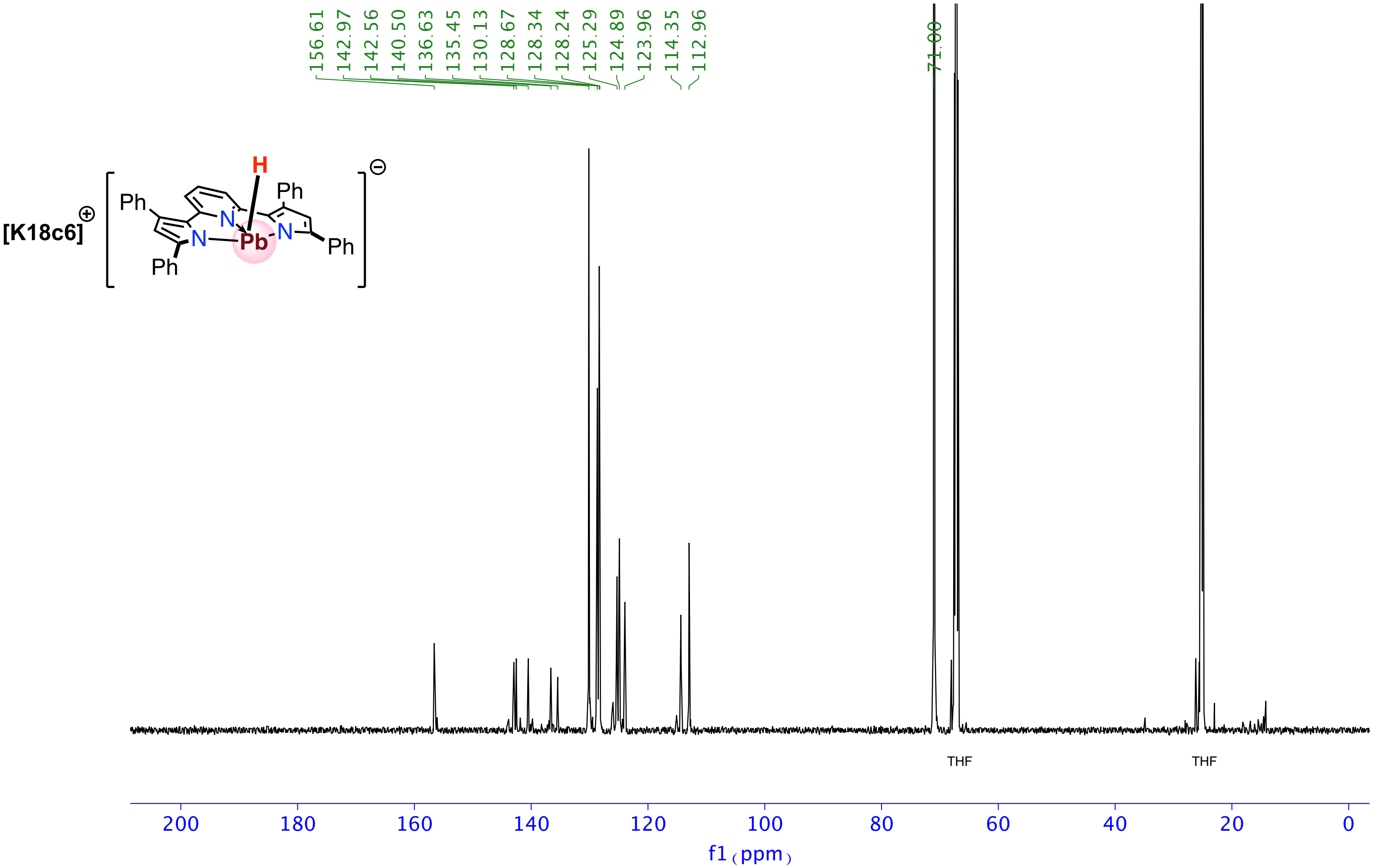

Figure S7. $^{13}C\{^1H\}$ NMR spectrum of **[K18c6][1-H]** (THF-d_8, 263K). Small amounts of **LK$_2$** can be detected due to decomposition of **[K18c6][1-H]**.

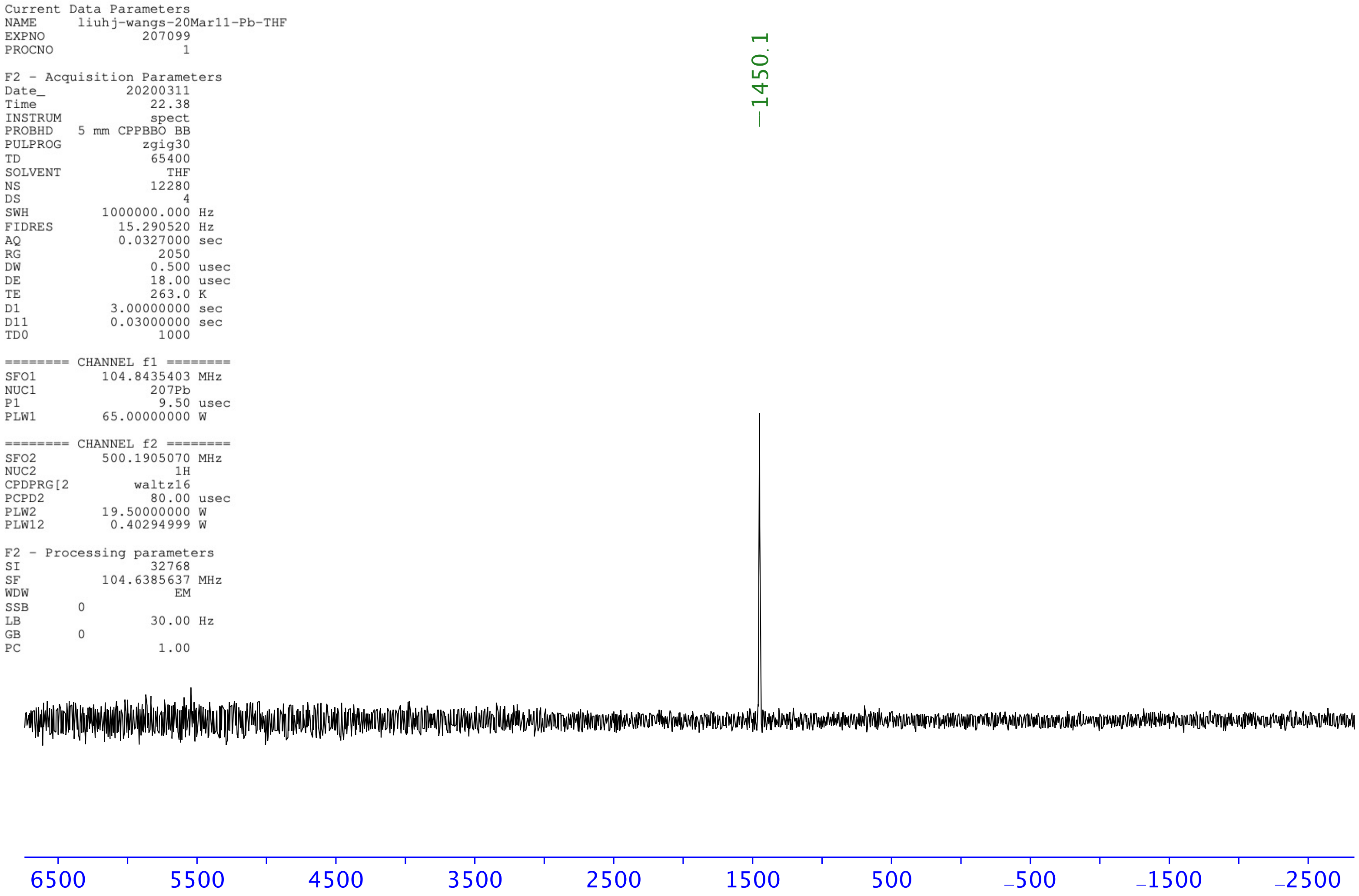

```
Current Data Parameters
NAME     liuhj-wangs-20Mar11-Pb-THF
EXPNO              207099
PROCNO                  1

F2 - Acquisition Parameters
Date_            20200311
Time                22.38
INSTRUM             spect
PROBHD   5 mm CPPBBO BB
PULPROG            zgig30
TD                  65400
SOLVENT               THF
NS                  12280
DS                      4
SWH           1000000.000 Hz
FIDRES          15.290520 Hz
AQ              0.0327000 sec
RG                   2050
DW                  0.500 usec
DE                  18.00 usec
TE                  263.0 K
D1             3.00000000 sec
D11            0.03000000 sec
TD0                  1000

======== CHANNEL f1 ========
SFO1          104.8435403 MHz
NUC1                207Pb
P1                   9.50 usec
PLW1          65.00000000 W

======== CHANNEL f2 ========
SFO2          500.1905070 MHz
NUC2                   1H
CPDPRG[2          waltz16
PCPD2               80.00 usec
PLW2          19.50000000 W
PLW12          0.40294999 W

F2 - Processing parameters
SI                  32768
SF            104.6385637 MHz
WDW                    EM
SSB      0
LB                  30.00 Hz
GB       0
PC                   1.00
```

Figure S8. ^{207}Pb{^{1}H} NMR spectrum of **[K18c6][1-H]** (THF-d_8, 263K)

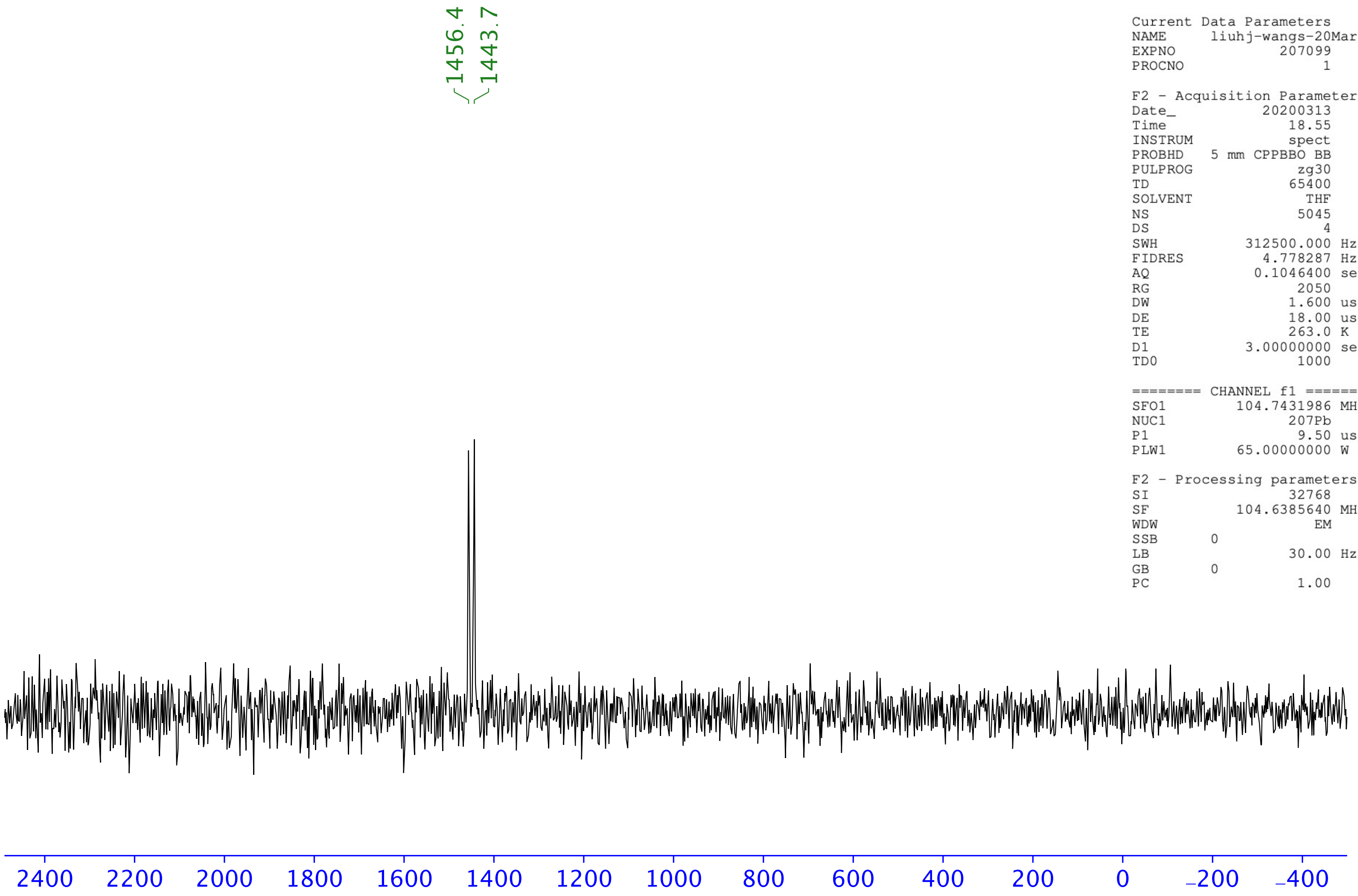

```
Current Data Parameters
NAME     liuhj-wangs-20Mar13-Pb-THF-263K
EXPNO              207099
PROCNO                  1

F2 - Acquisition Parameters
Date_            20200313
Time                18.55
INSTRUM             spect
PROBHD   5 mm CPPBBO BB
PULPROG              zg30
TD                  65400
SOLVENT               THF
NS                   5045
DS                      4
SWH            312500.000 Hz
FIDRES           4.778287 Hz
AQ              0.1046400 sec
RG                   2050
DW                  1.600 usec
DE                  18.00 usec
TE                  263.0 K
D1             3.00000000 sec
TD0                  1000

======== CHANNEL f1 ========
SFO1         104.7431986 MHz
NUC1                207Pb
P1                   9.50 usec
PLW1          65.00000000 W

F2 - Processing parameters
SI                  32768
SF           104.6385640 MHz
WDW                    EM
SSB      0
LB                  30.00 Hz
GB       0
PC                   1.00
```

Figure S9. The proton-coupled ^{207}Pb NMR spectrum of **[K18c6][1-H]** (THF-d_8, 263K)

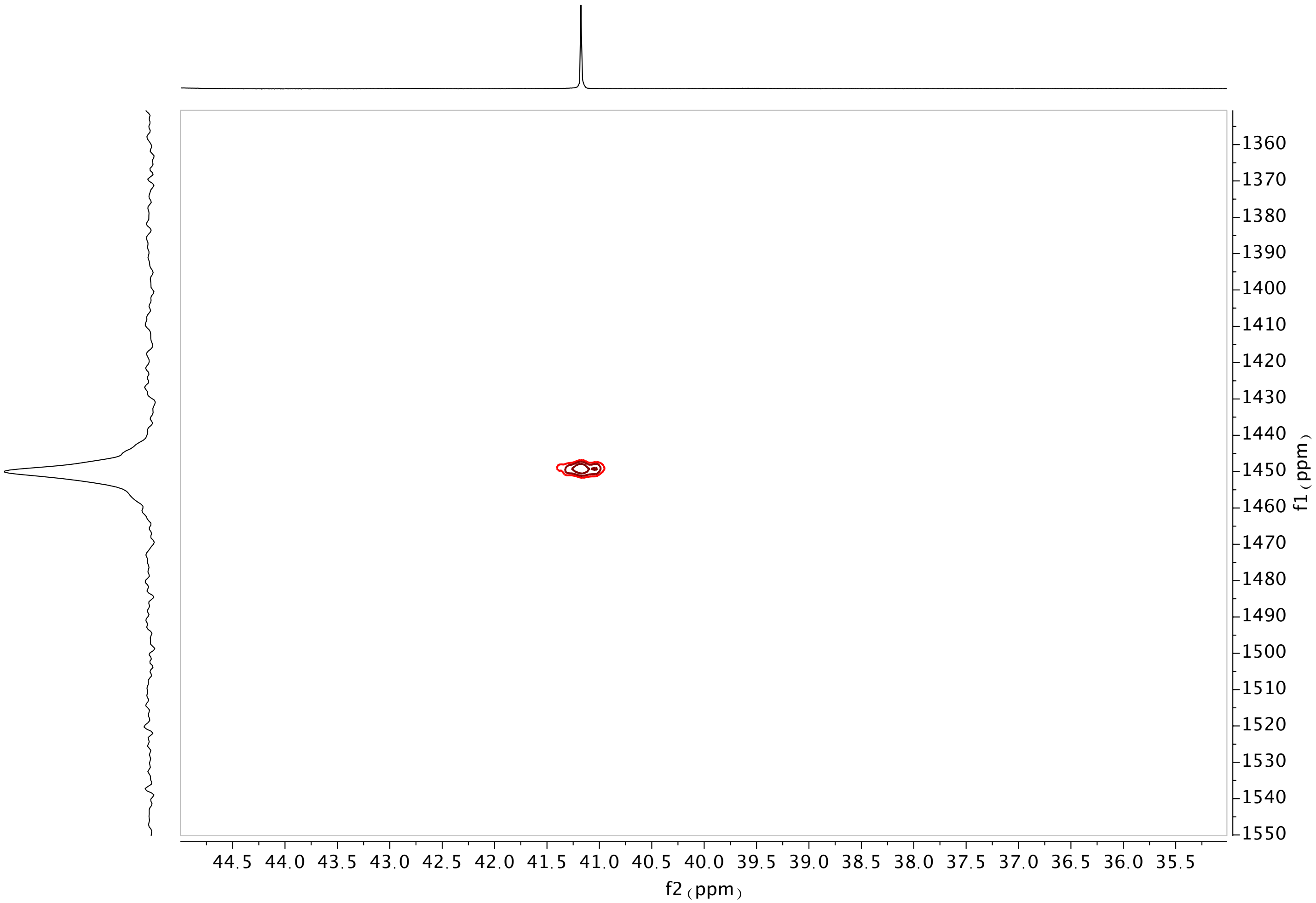

```
NAME                 Wong
EXPNO                   2
PROCNO                  1
Date_            20210324
Time                11.51 h
INSTRUM             spect
PROBHD     Z116098_0102 (
PULPROG          hmqcgpqf
TD                   2048
SOLVENT               THF
NS                     16
DS                     16
RO                      0
SWH              4000.000 Hz
FIDRES           3.906250 Hz
AQ              0.2560500 sec
RG                 202.42
DW                125.000 usec
DE                   6.50 usec
TE                  252.9 K
CNST2        1300.0000000
D0             0.00000300 sec
D1             2.00000000 sec
D2             0.00038462 sec
D12            0.00002000 sec
D13            0.00000400 sec
D16            0.00020000 sec
IN0            0.00002980 sec
ND0                     2
TD                     61
SFO1             83.83097 MHz
FIDRES         275.057770 Hz
SW                200.147 ppm
FnMODE                 QF
SI                   1024
SF            400.1300000 MHz
WDW                    EM
SSB                     0
LB                  20.00 Hz
GB                      0
PC                   1.40
SI                   1024
MC2                    QF
SF             83.7095930 MHz
WDW                    EM
SSB                     0
LB                  20.00 Hz
GB                      0
```

Figure S10. ^{1}H-^{207}Pb HMQC NMR spectrum of **[K18c6][1-H]** (THF-d_8, 253K)

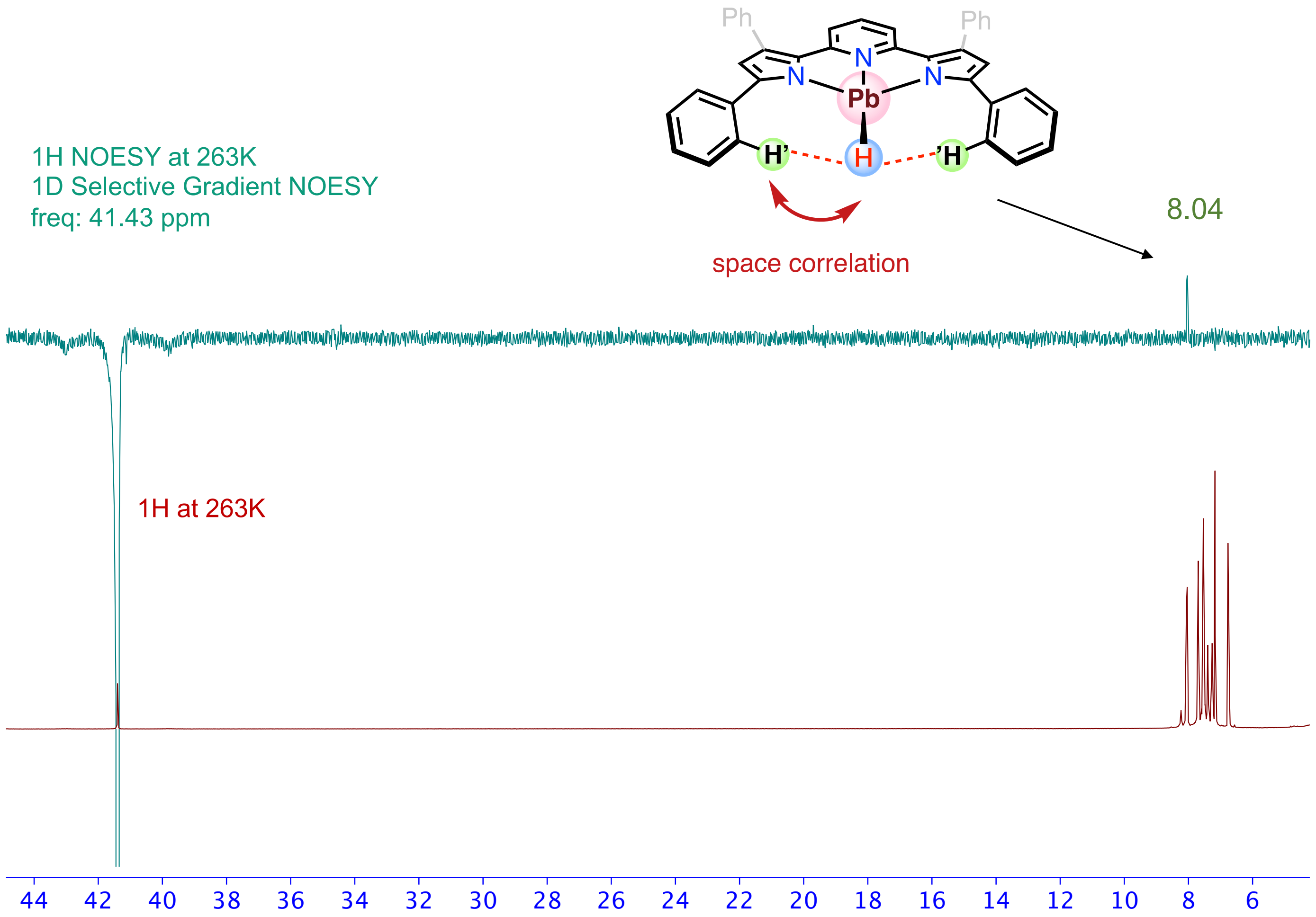

Figure S11. The stacked 1D ^{1}H NOESY spectrum (top) and ^{1}H NMR spectrum (bottom) of **[K18c6][1-H]** (THF-d_8, 263K).

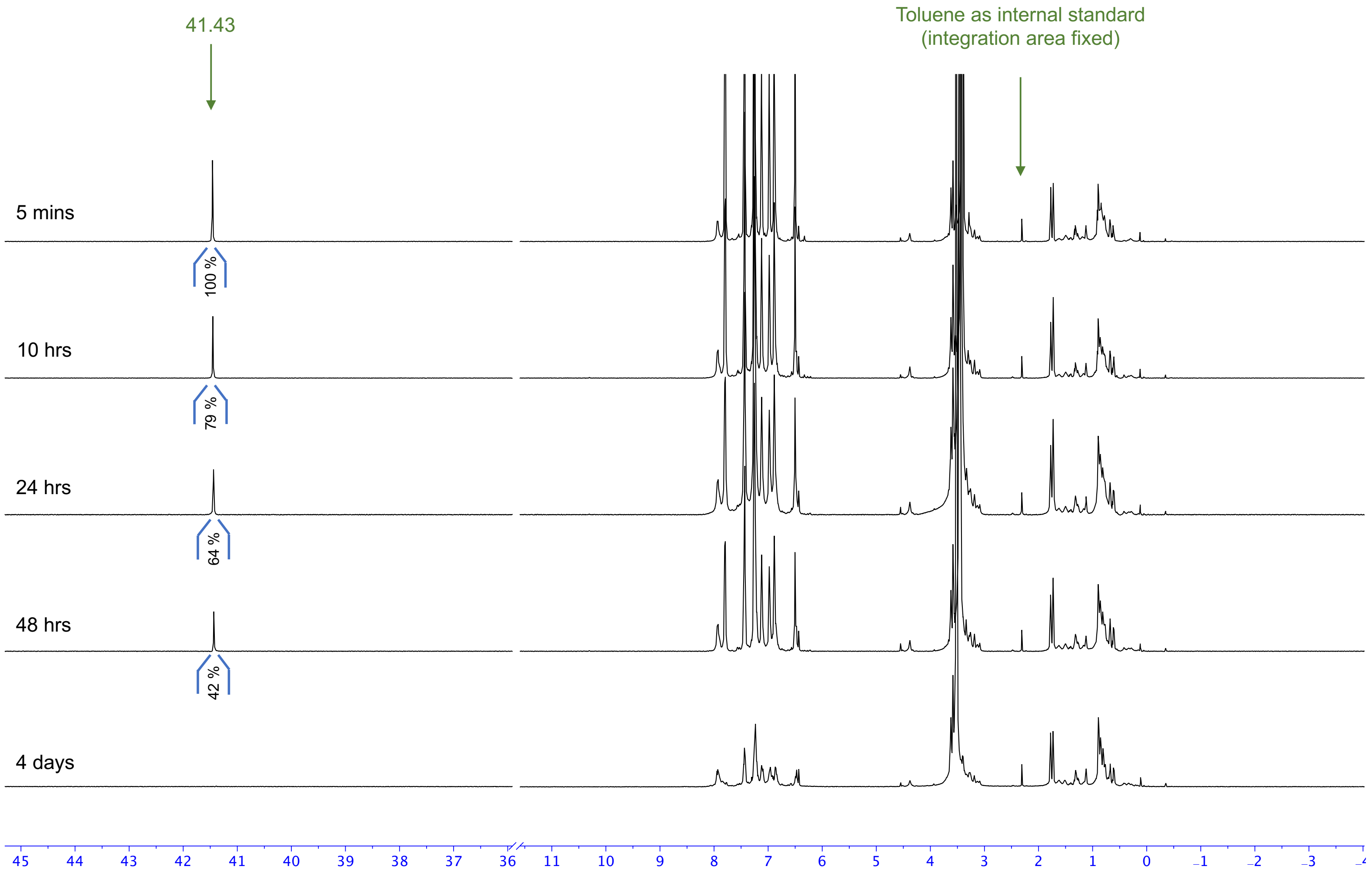

Figure S12: Decomposition reaction of **[K18c6][1-H]** monitored by ^{1}H NMR spectroscopy over 4 days at ambient temperature using residual toluene as the internal standard (THF-d_8, 298K).

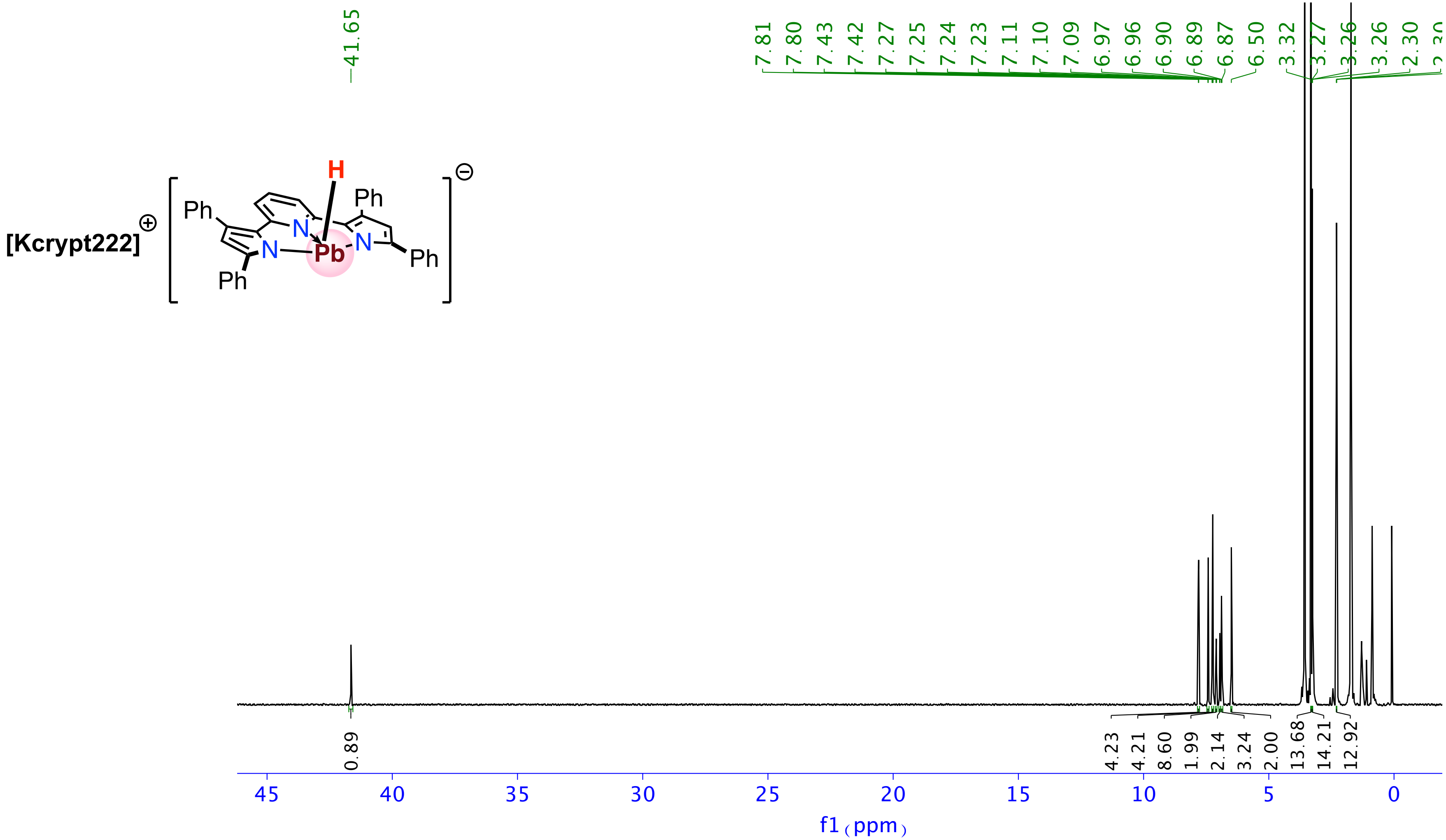

Figure S13. ^{1}H NMR spectrum of **[Kcrypt222][1-H]** (THF-d_8, 263K)

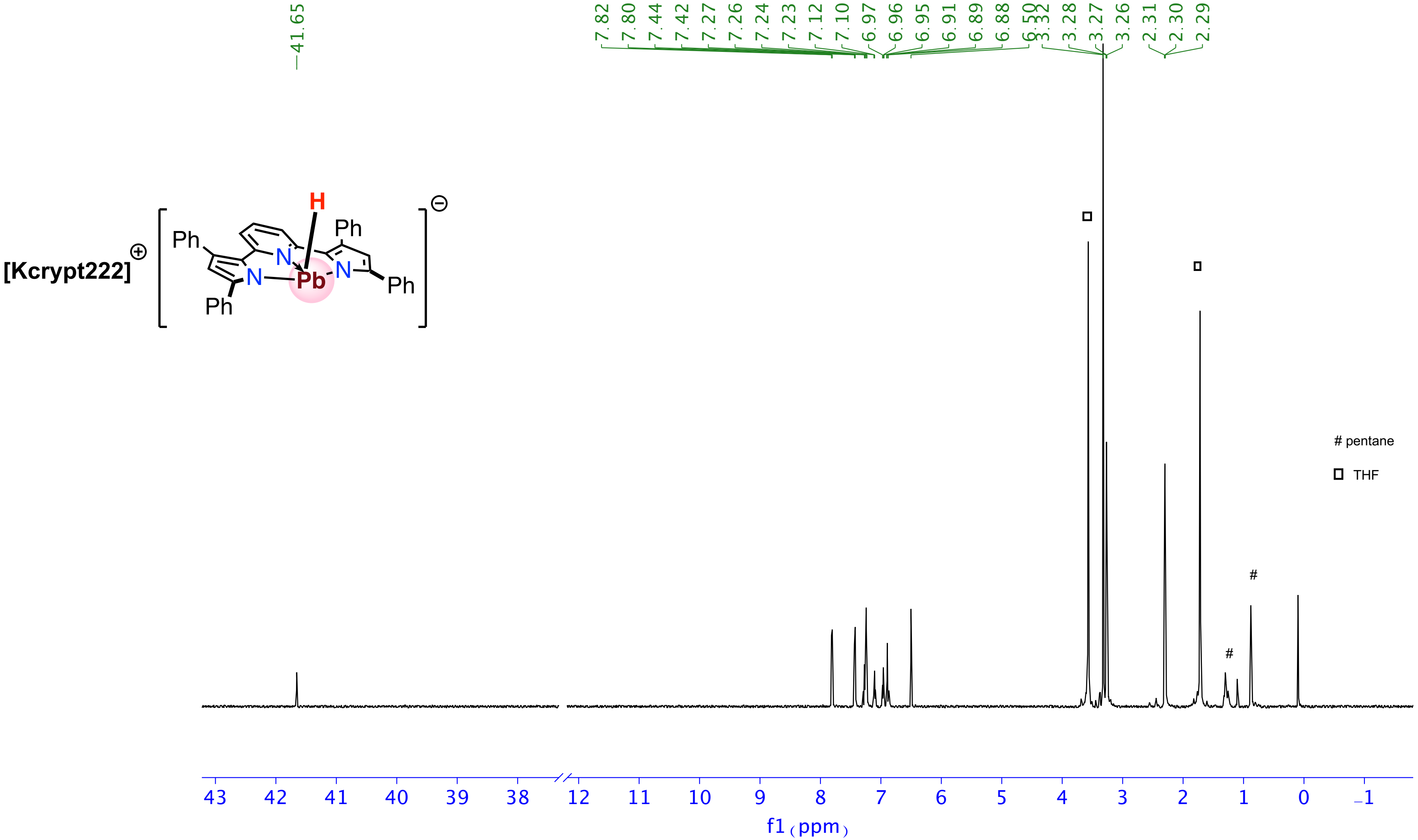

Figure S14. The enlarged part of the ^{1}H NMR spectrum of **[Kcrypt222][1-H]** (THF-d_8, 263K)

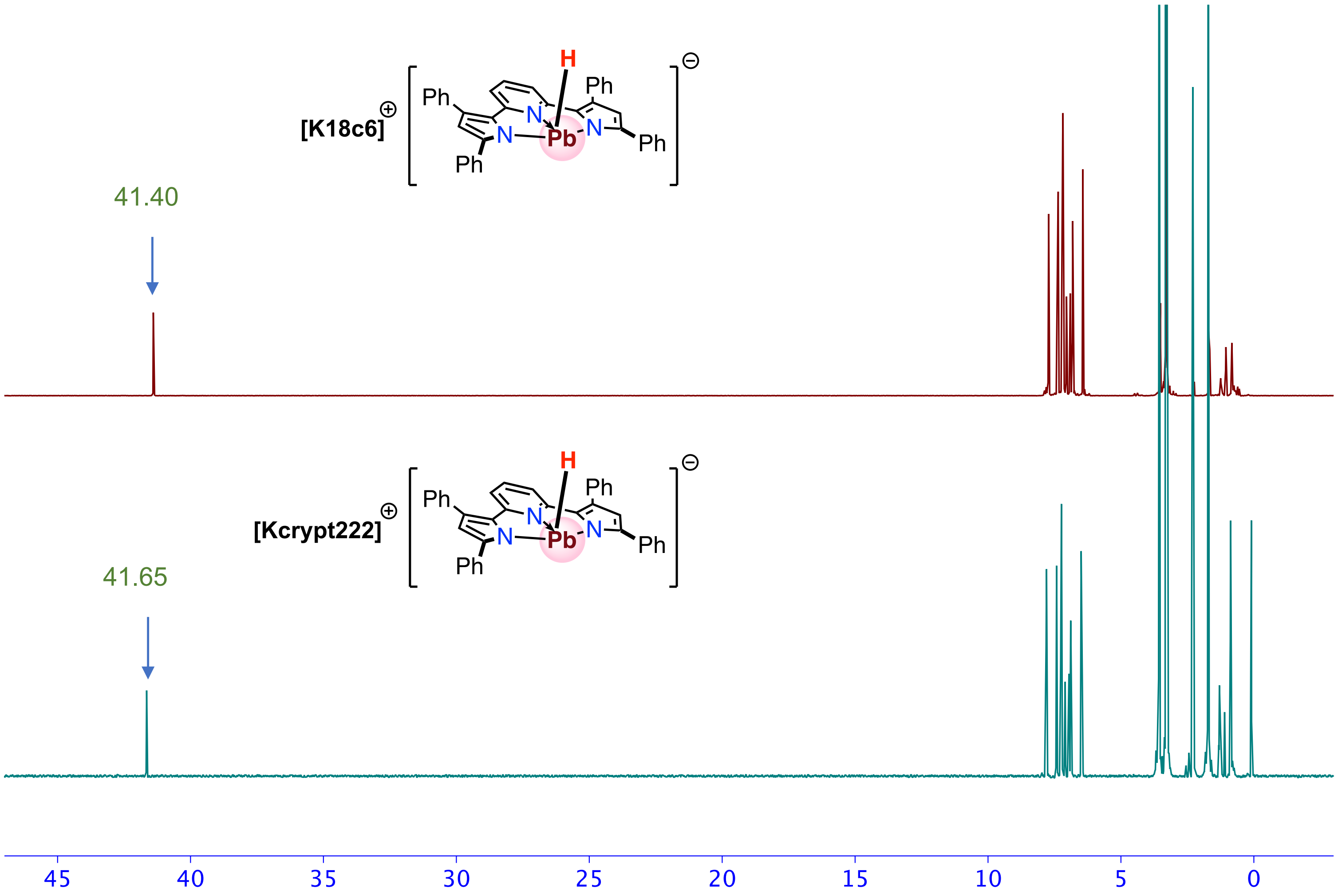

Figure S15. The stacked ^{1}H NMR spectra of **[K18c6][1-H]** (top) and **[Kcrypt222][1-H]** (bottom) (THF-d_8, 263K)

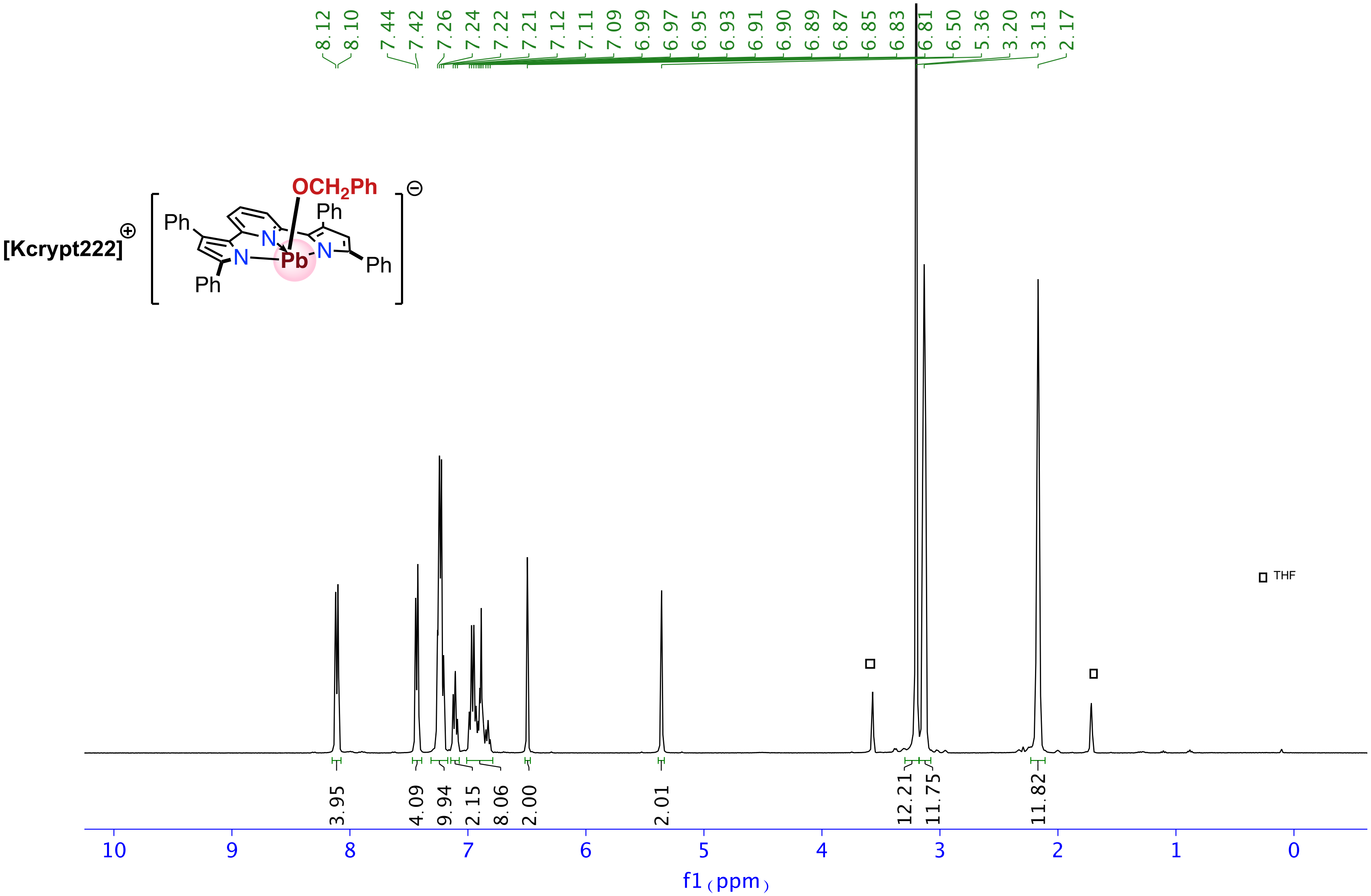

Figure S16. ^{1}H NMR spectrum of **[Kcrypt222][1-OBz]** (THF-d_8, 298K)

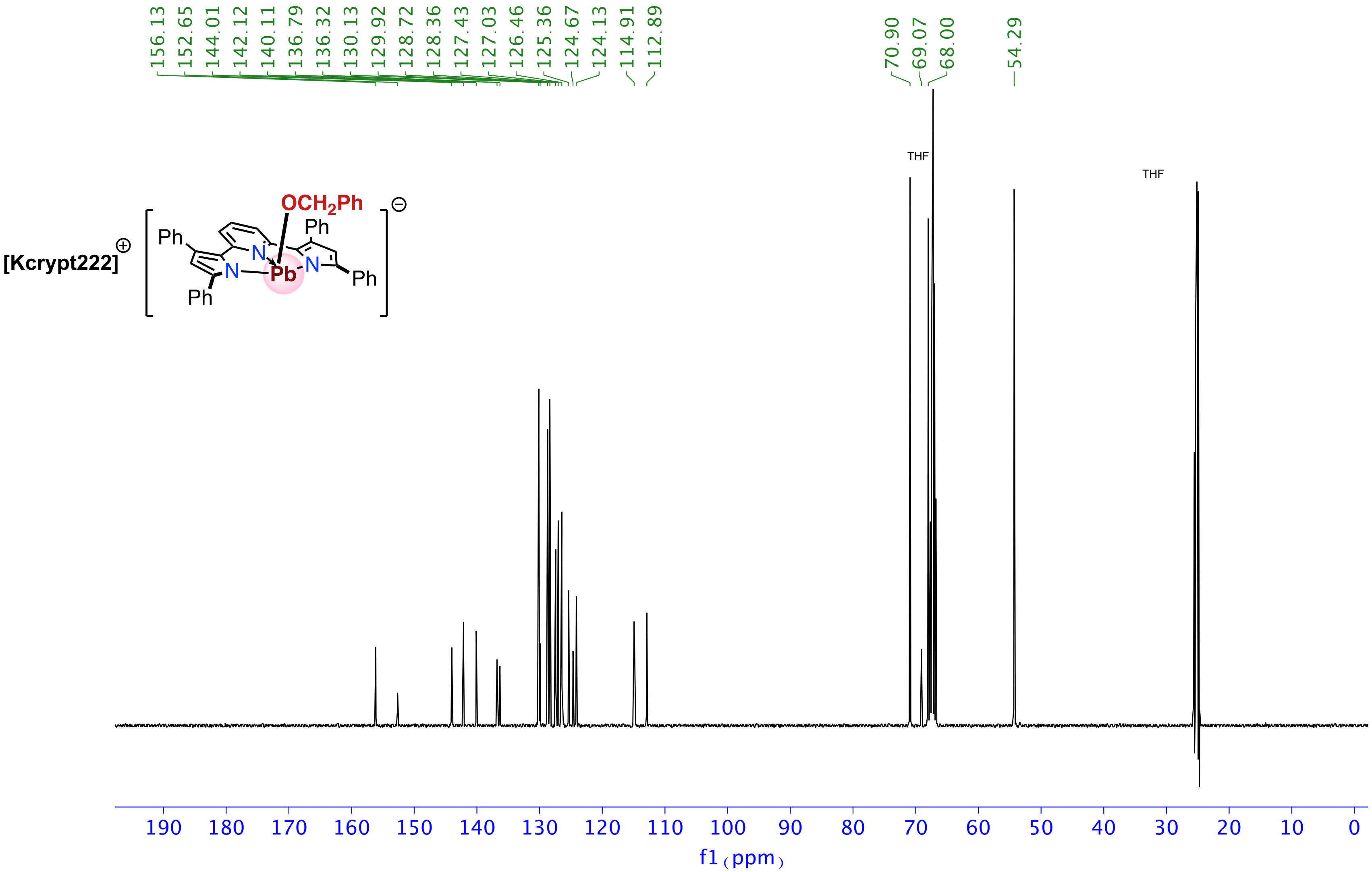

Figure S17. ^{13}C{^{1}H} NMR spectrum of **[Kcrypt222][1-OBz]** (THF-d_8, 298K)

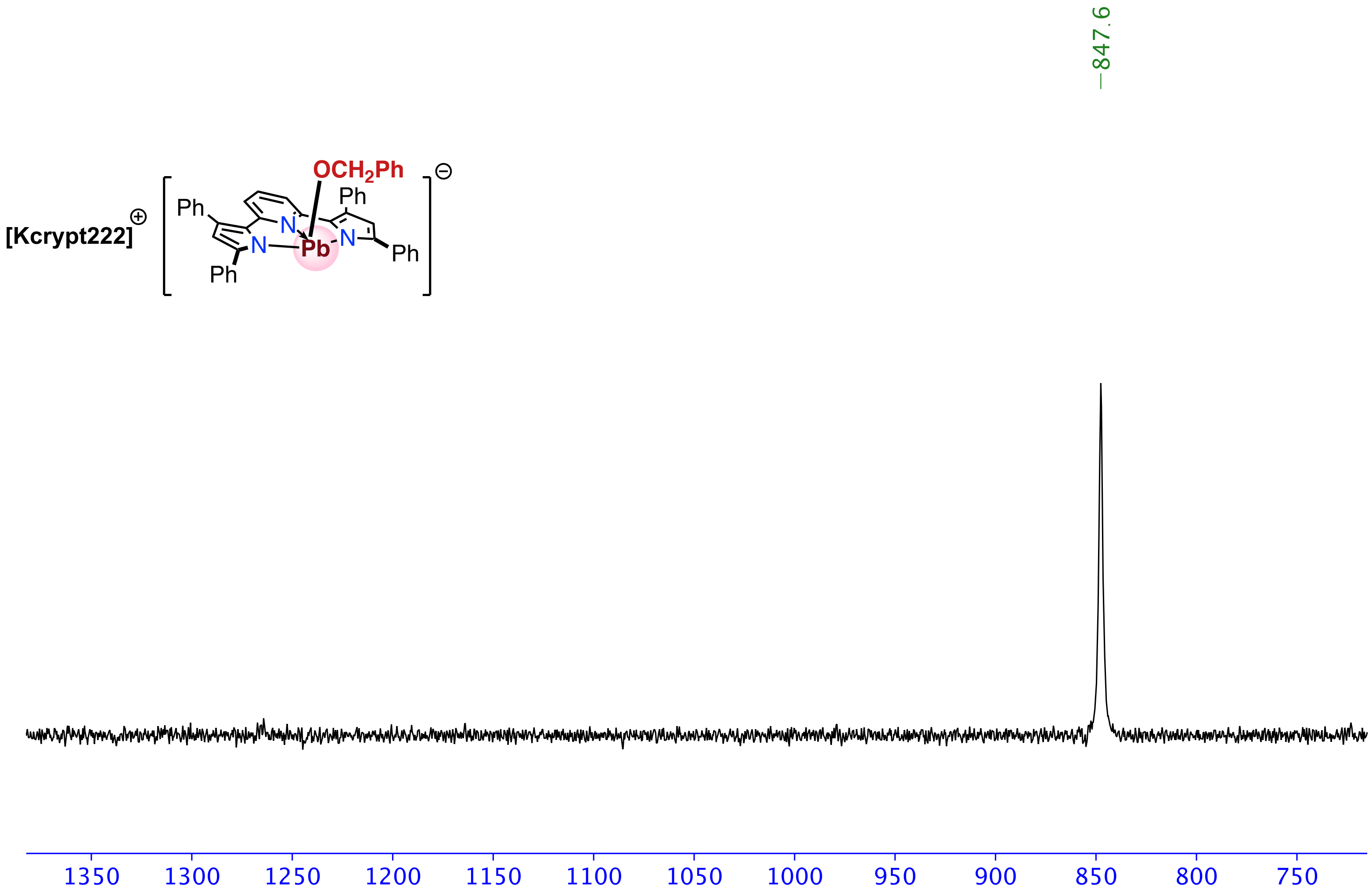

Figure S18. ^{207}Pb{^{1}H} NMR spectrum of **[Kcrypt222][1-OBz]** (THF-d_8, 298K)

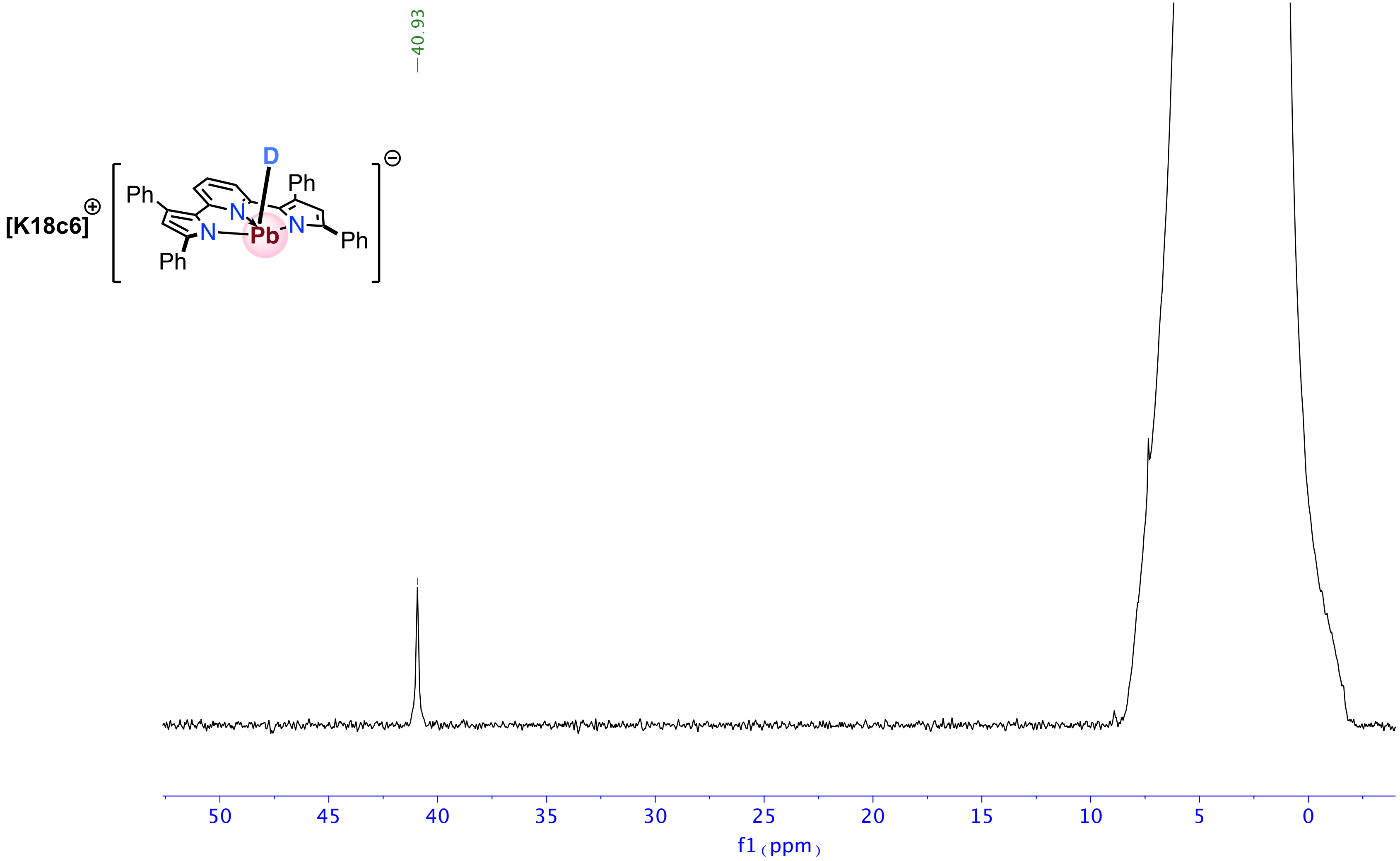

Figure S19. ^{2}H NMR spectrum of **[K18c6][1-D]** (THF-d_8, 263K)

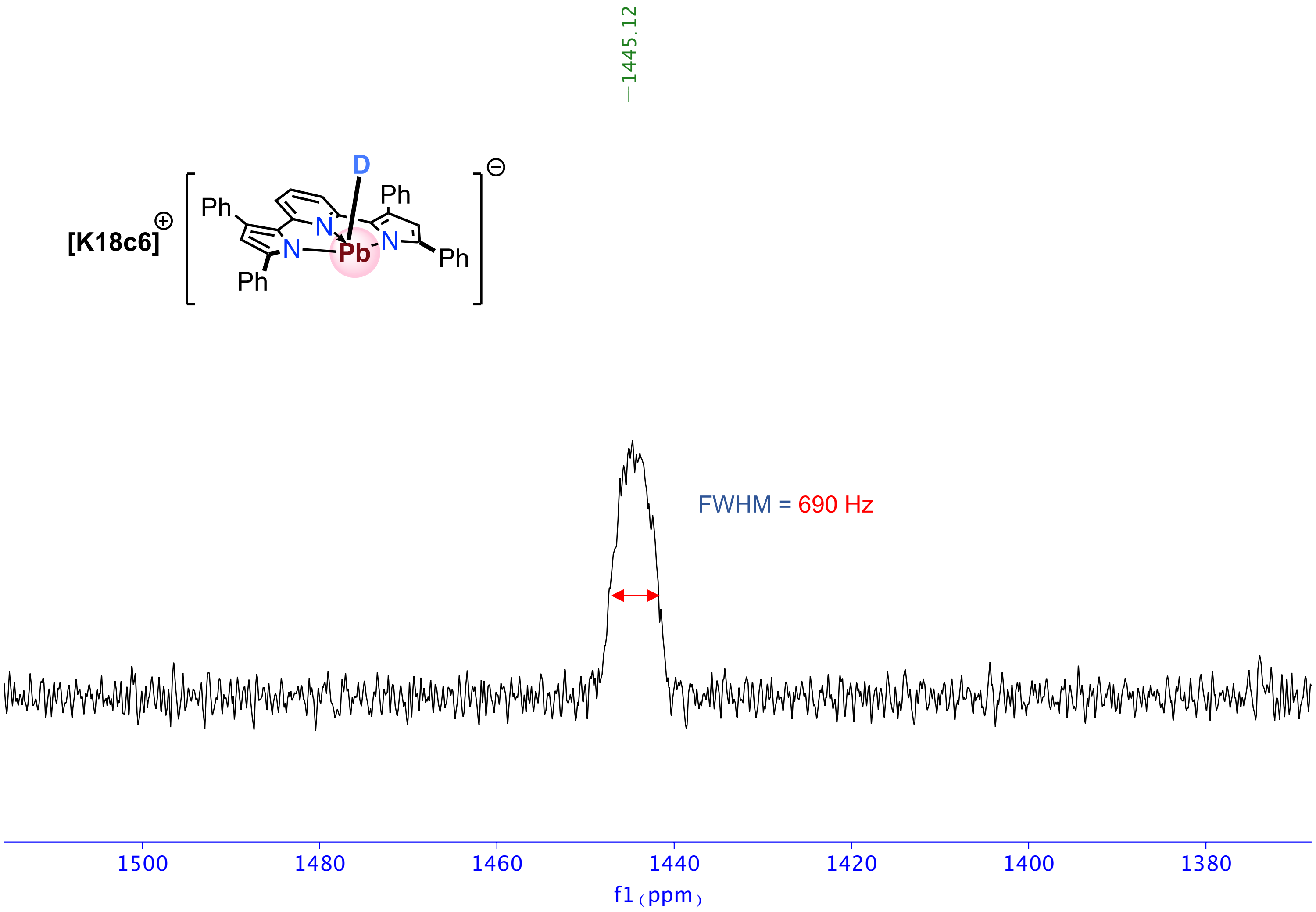

Figure S20. ^{207}Pb{^{1}H} NMR spectrum of **[K18c6][1-D]** (THF-d_8, 263K)

1.3 IR spectrum of [Kcrypt222][1-H] and [Kcrypt222][1-D].

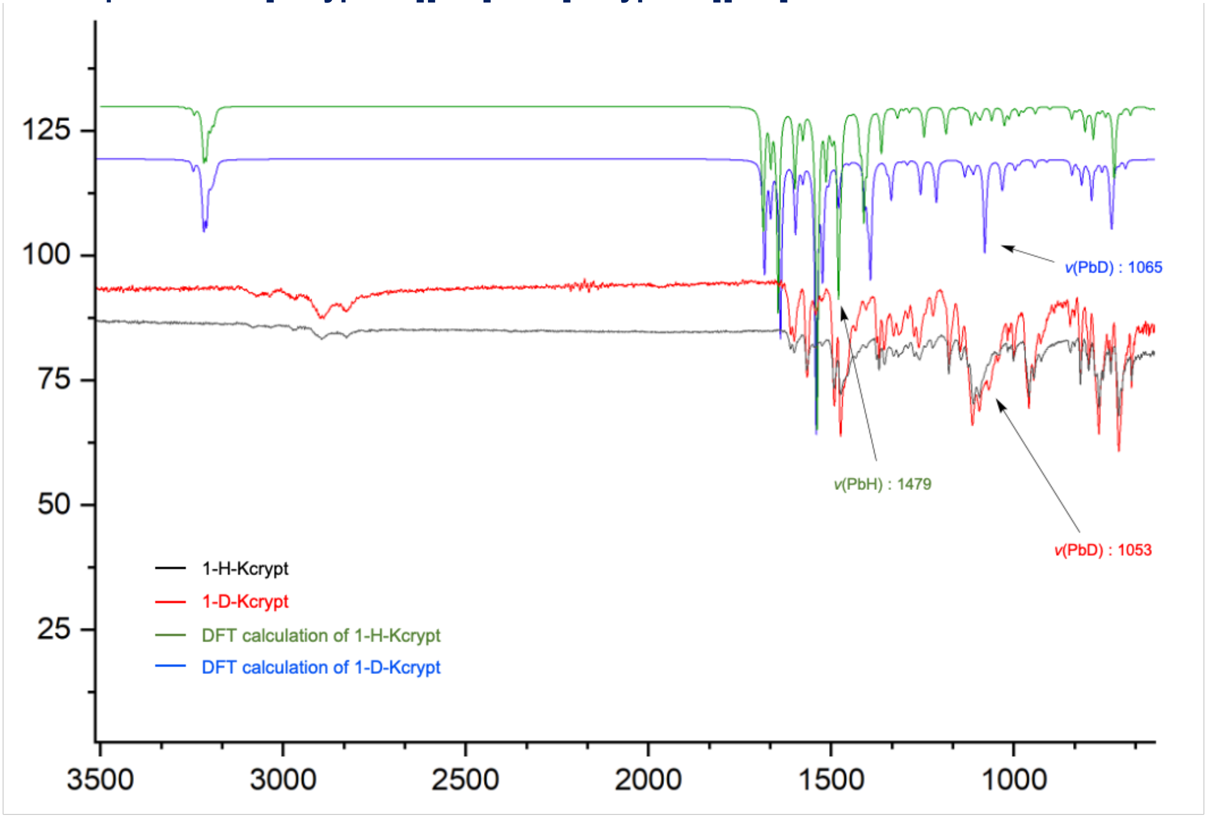

Figure S21. The overlapped IR spectrum of **[Kcrypt222][1-H]** and **[Kcrypt222][1-D]**.

The IR bands predicted by DFT calculations appear closely to those of the experimental spectra. DFT calculations of **[1-H]**$^-$ and **[1-D]**$^-$ reveal ν_{PbH} and ν_{PbD} at 1479 cm^{-1} and 1065 cm^{-1}, respectively. The ν_{PbH} of **[Kcrypt222][1-H]** is likely overlapped with other vibrational bands. The spectrum of **[Kcrypt222][1-D]** shows the Pb–D stretching band at 1053 cm^{-1}.

2. Details of ESI(–)-MS measurements and data analysis

A Thermo Scientific LTQ XL linear ion trap mass spectrometer performed the analysis in this work. The samples were pumped using a Thermo Scientific Surveyor MS pump delivering 3 μL /min to electrospray ionization (ESI) source. Each spectrum was acquired 60 scans in negative mode. An ESI voltage of -4.8 kV was applied, combining with the tube lens in -40 V, and the temperature of the ion transfer tube was set to 275 °C. To avoid the samples reacting with oxygen or water vapor, they were transferred to the syringe in a glove box, and the ionization region was purged with nitrogen. The spectra were fitted with the theoretical isotope distributions to confirm the elementary composition of detected ion.

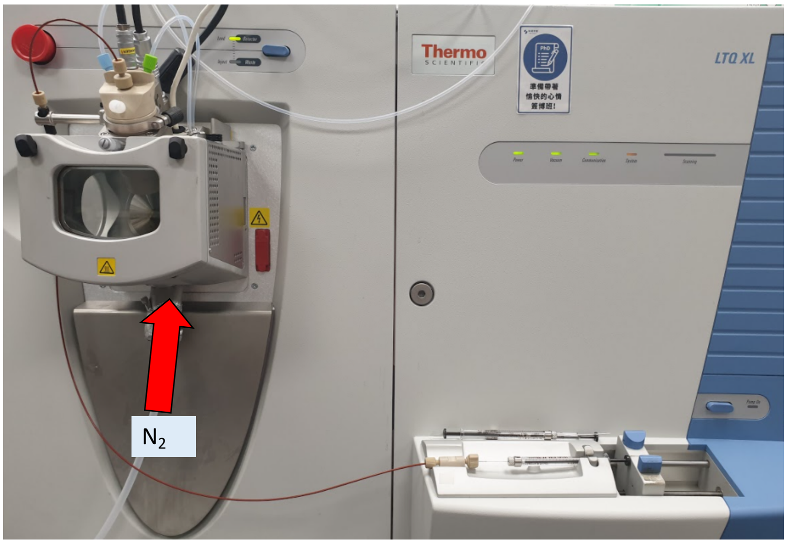

Figure S22. The ESI mass spectrometer.

2.1 ESI(–)MS Data for [1-H]$^-$ and [1-D]$^-$.

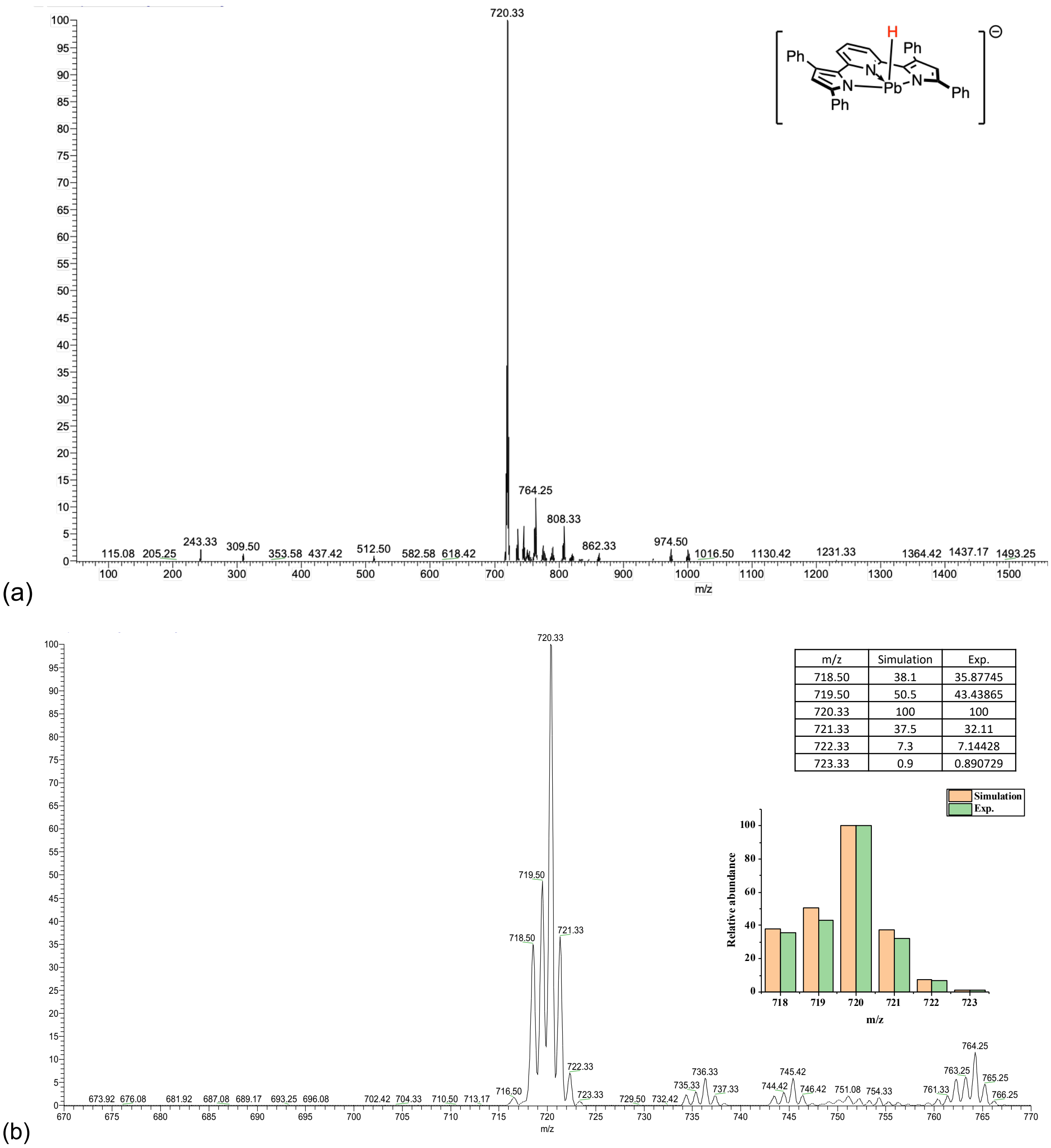

m/z	Simulation	Exp.
718.50	38.1	35.87745
719.50	50.5	43.43865
720.33	100	100
721.33	37.5	32.11
722.33	7.3	7.14428
723.33	0.9	0.890729

Figure S23. (a) ESI-MS(–) spectrum **[1-H]**$^-$. (b) The enlarged part of **[1-H]**$^-$ ion signal and the inset shows the normalized comparison of experimental and simulated isotope distributions.

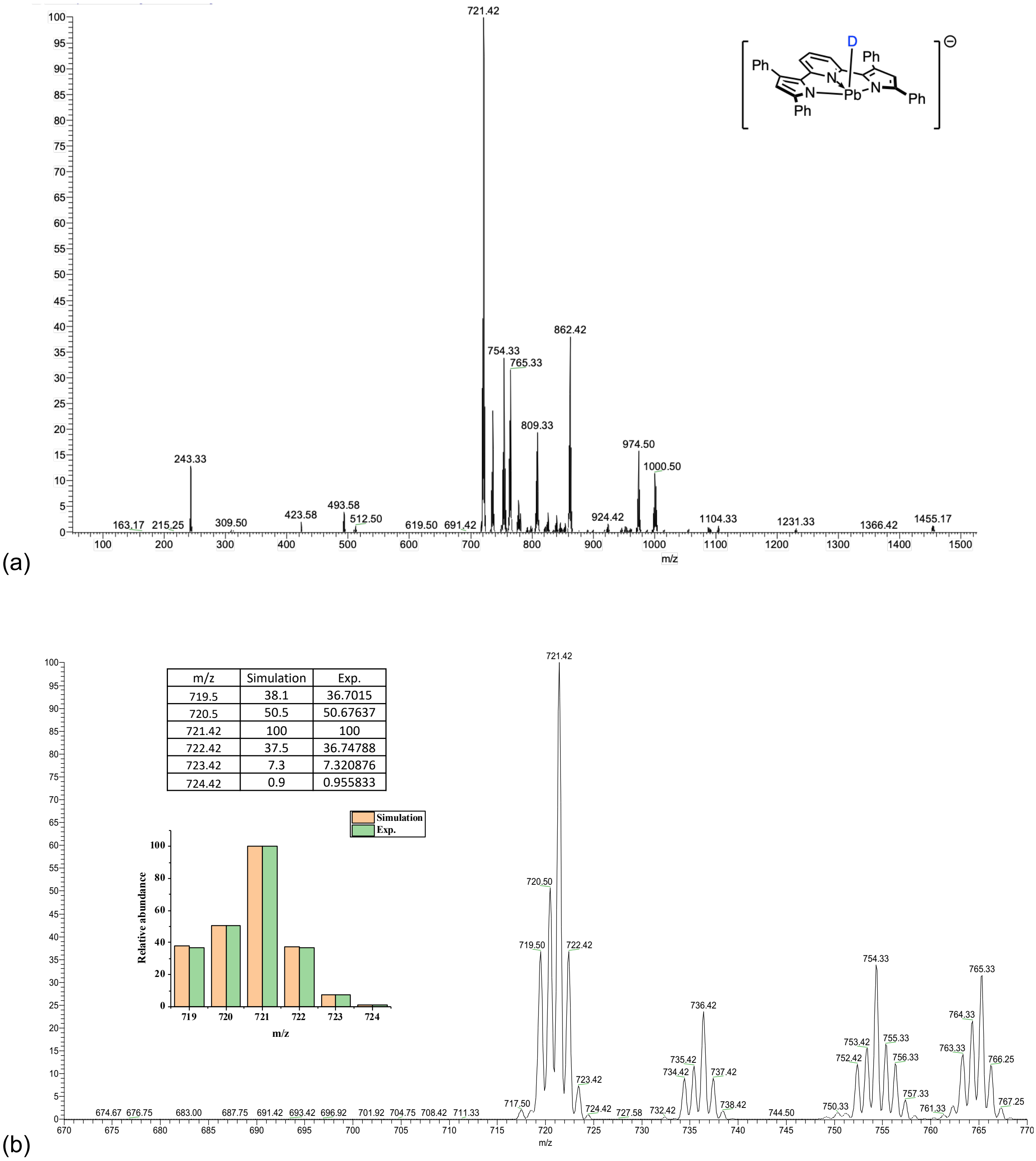

m/z	Simulation	Exp.
719.5	38.1	36.7015
720.5	50.5	50.67637
721.42	100	100
722.42	37.5	36.74788
723.42	7.3	7.320876
724.42	0.9	0.955833

Figure S24. (a) ESI-MS(–) spectrum **[1-D]**⁻. (b) The enlarged part of **[1-D]**⁻ ion signal and the inset shows the normalized comparison of experimental and simulated results isotope distributions.

3. Single-crystal X-ray diffraction crystal structure figures and data tables

Single-crystal X-ray diffraction were performed on a Bruker APEX DUO diffractometer with APEX II 4K and multi-layer mirror monochromated Mo K_α radiation (λ = 0.71073 Å) at 200(2) K. Data collection and reduction were performed with Bruker APEX II software. All of non-hydrogen atoms are refined anisotropically. Hydrogen atoms attached to the carbons were fixed at calculated positions and refined using a riding mode. Multiple disordered solvent molecules were observed in the crystal structures of all complexes. Whenever possible, co-crystallizing solvent molecules were modeled. Otherwise, SQUEEZE was employed to treat diffuse solvent contribution in the voids.

Table S1. Crystal data and structure refinement for **1-THF$_2$** (one THF squeezed)

Empirical formula	$C_{45}H_{41}N_3O_2Pb$	
Formula weight	863.00	
Temperature	200(2) K	
Wavelength	0.71073 Å	
Crystal system	Monoclinic	
Space group	P 21/c	
Unit cell dimensions	a = 15.785(2) Å	α= 90°.
	b = 14.4681(18) Å	β= 91.067(3)°.
	c = 21.038(3) Å	γ = 90°.
Volume	4804.0(11) Å^3	
Z	4	
Density (calculated)	1.193 Mg/m^3	
Absorption coefficient	3.544 mm^{-1}	
F(000)	1720	
Crystal size	0.32 x 0.27 x 0.11 mm^3	
Theta range for data collection	2.13 to 25.23°.	
Index ranges	-18<=h<=17, -17<=k<=17, -24<=l<=25	
Reflections collected	70371	
Independent reflections	8608 [R(int) = 0.0774]	
Completeness to theta = 25.23°	99.2 %	
Absorption correction	multi-scan	
Max. and min. transmission	0.6965 and 0.3967	
Refinement method	Full-matrix least-squares on F^2	
Data / restraints / parameters	8608 / 56 / 430	
Goodness-of-fit on F2	1.020	
Final R indices [I>2sigma(I)]	R1 = 0.0734, wR2 = 0.2047	
R indices (all data)	R1 = 0.1022, wR2 = 0.2181	
Largest diff. peak and hole	2.006 and -1.817 e/Å^{-3}	

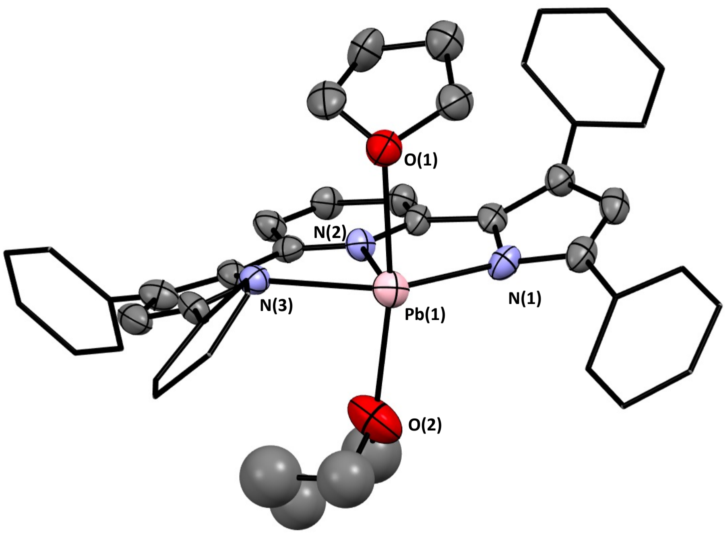

Figure S25. ORTEP diagram of **1-THF$_2$** (30% thermal ellipsoids; hydrogen atoms omitted). Selected interatomic distances (Å) and angles (°): N(1)–Pb(1) 2.456(9), N(2)–Pb(1) 2.401(7), N(3)–Pb(1) 2.440(8), Pb(1)–O(1) 2.547(8), Pb(1)–O(2) 2.528(12); N(1)–Pb(1)–N(2) 67.8(3), N(2)–Pb(1)–N(3) 67.7(3), N(1)–Pb(1)–N(3) 135.4(3), N(1)–Pb(1)–O(1) 88.0(3), N(2)–Pb(1)–O(1) 82.1(3), N(3)–Pb(1)–O(1) 85.4(3), N(1)–Pb(1)–O(2) 92.4(3), N(2)–Pb(1)–O(2) 84.3(4), N(3)–Pb(1)–O(2) 83.9(4), O(1)–Pb(1)–O(2) 165.1(4).

Table S2. Crystal data and structure refinement for **[Kcrypt222][1-H]**

Empirical formula	$C_{55}H_{61}KN_5O_6Pb$	
Formula weight	1134.38	
Temperature	200(2) K	
Wavelength	0.71073 Å	
Crystal system	Monoclinic	
Space group	P 21/n	
Unit cell dimensions	a = 14.2258(4) Å	α = 90°.
	b = 18.3607(5) Å	β = 100.4360(10)°.
	c = 19.9771(5) Å	γ = 90°.
Volume	5131.6(2) $Å^3$	
Z	4	
Density (calculated)	1.468 Mg/m^3	
Absorption coefficient	3.423 mm^{-1}	
F(000)	2300	
Crystal size	0.39 x 0.30 x 0.20 mm^3	
Theta range for data collection	2.22 to 25.10°.	
Index ranges	-16<=h<=16, -21<=k<=21, -19<=l<=23	
Reflections collected	51385	
Independent reflections	9112 [R(int) = 0.0563]	
Completeness to theta = 25.10°	99.7 %	
Absorption correction	multi-scan	
Max. and min. transmission	0.5476 and 0.3487	
Refinement method	Full-matrix least-squares on F^2	
Data / restraints / parameters	9112 / 0 / 612	
Goodness-of-fit on F2	1.290	
Final R indices [I>2sigma(I)]	R1 = 0.0687, wR2 = 0.1325	
R indices (all data)	R1 = 0.0796, wR2 = 0.1362	
Largest diff. peak and hole	1.485 and -3.134 $e/Å^{-3}$	

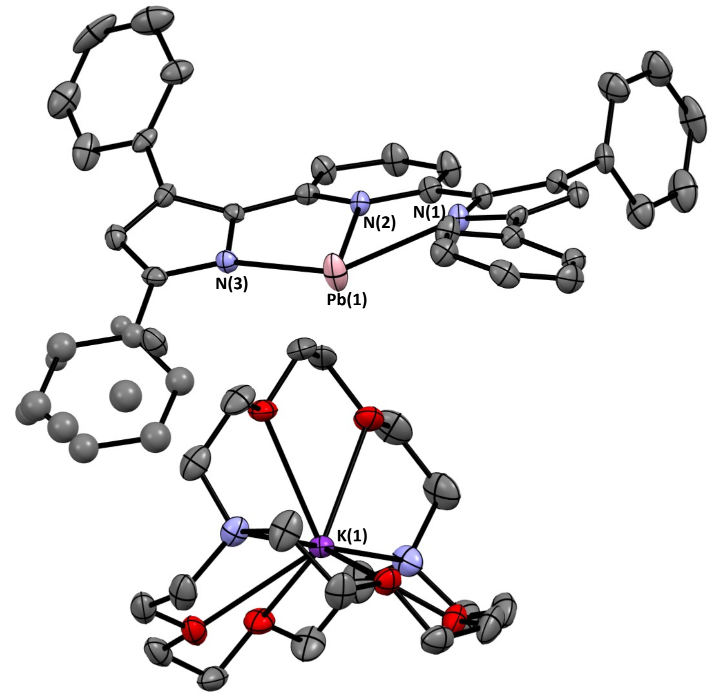

Figure S26a. ORTEP of molecular structure of **[Kcrypt222][1-H]**. Thermal ellipsoids are shown at 30% probability level and hydrogen atoms have been omitted for clarity. Selected interatomic distances (Å) and angles (º): N(1)–Pb(1) 2.480(6), N(2)–Pb(1) 2.397(6), N(3)–Pb(1) 2.474(6); N(1)–Pb(1)–N(2) 68.30(2), N(2)–Pb(1)–N(3) 68.47(19), N(1)–Pb(1)–N(3) 136.30(2).

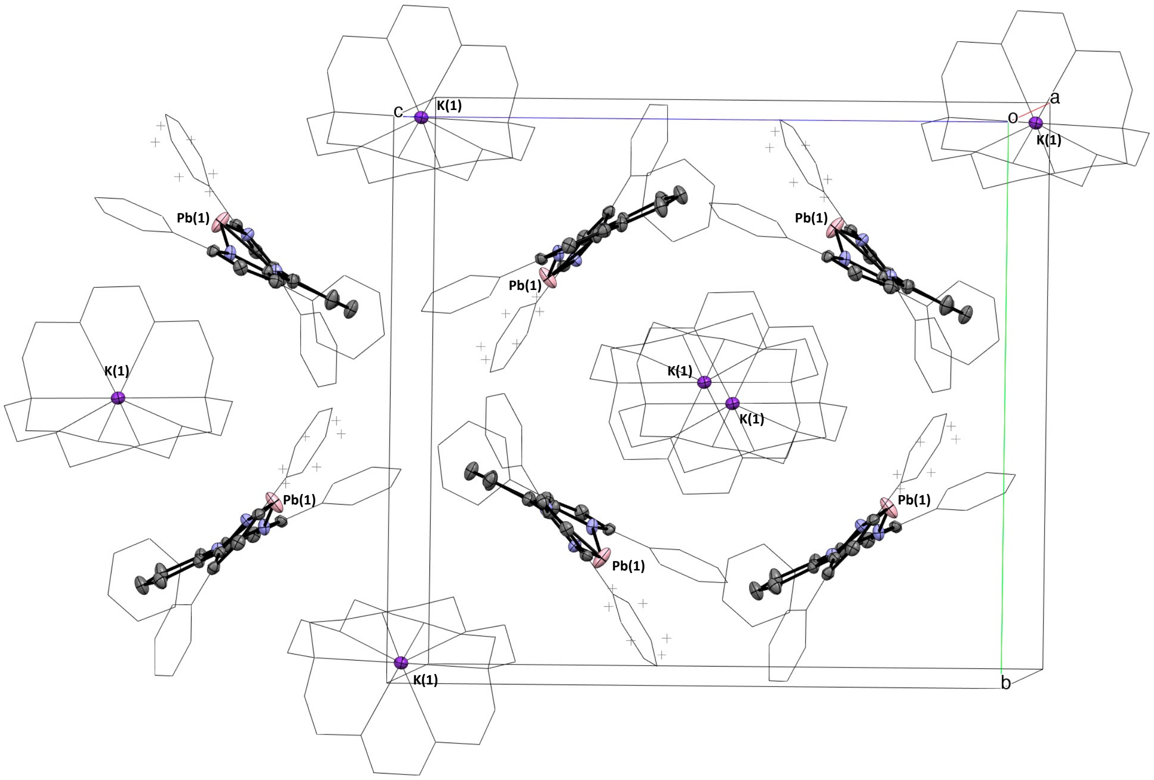

Figure S26b. Crystal packing diagram of **[Kcrypt222][1-H]** (30% thermal ellipsoids; hydrogen atoms omitted for clarity).

Table S3. Crystal data and structure refinement for **[Kcrypt222][1-OBz]**

Empirical formula	$C_{130}H_{142}K_2N_{10}O_{14}Pb_2$	
Formula weight	2561.12	
Temperature	200(2) K	
Wavelength	0.71073 Å	
Crystal system	Monoclinic	
Space group	P 21/c	
Unit cell dimensions	a = 14.4354(4) Å	a= 90°.
	b = 29.6617(9) Å	b= 103.1340(10)°.
	c = 28.4501(9) Å	g = 90°.
Volume	11863.1(6) $Å^3$	
Z	4	
Density (calculated)	1.434 Mg/m^3	
Absorption coefficient	2.972 mm^{-1}	
F(000)	5224	
Crystal size	0.22 x 0.14 x 0.02 mm^3	
Theta range for data collection	2.19 to 25.05°.	
Index ranges	-16<=h<=17, -35<=k<=35, -33<=l<=33	
Reflections collected	220399	
Independent reflections	20992 [R(int) = 0.1083]	
Completeness to theta = 25.05°	99.8 %	
Absorption correction	multi-scan	
Max. and min. transmission	0.9430 and 0.5609	
Refinement method	Full-matrix least-squares on F^2	
Data / restraints / parameters	20992 / 0 / 1417	
Goodness-of-fit on F2	1.029	
Final R indices [I>2sigma(I)]	R1 = 0.0385, wR2 = 0.0682	
R indices (all data)	R1 = 0.0733, wR2 = 0.0795	
Largest diff. peak and hole	1.862 and -1.785 e.$Å^{-3}$	

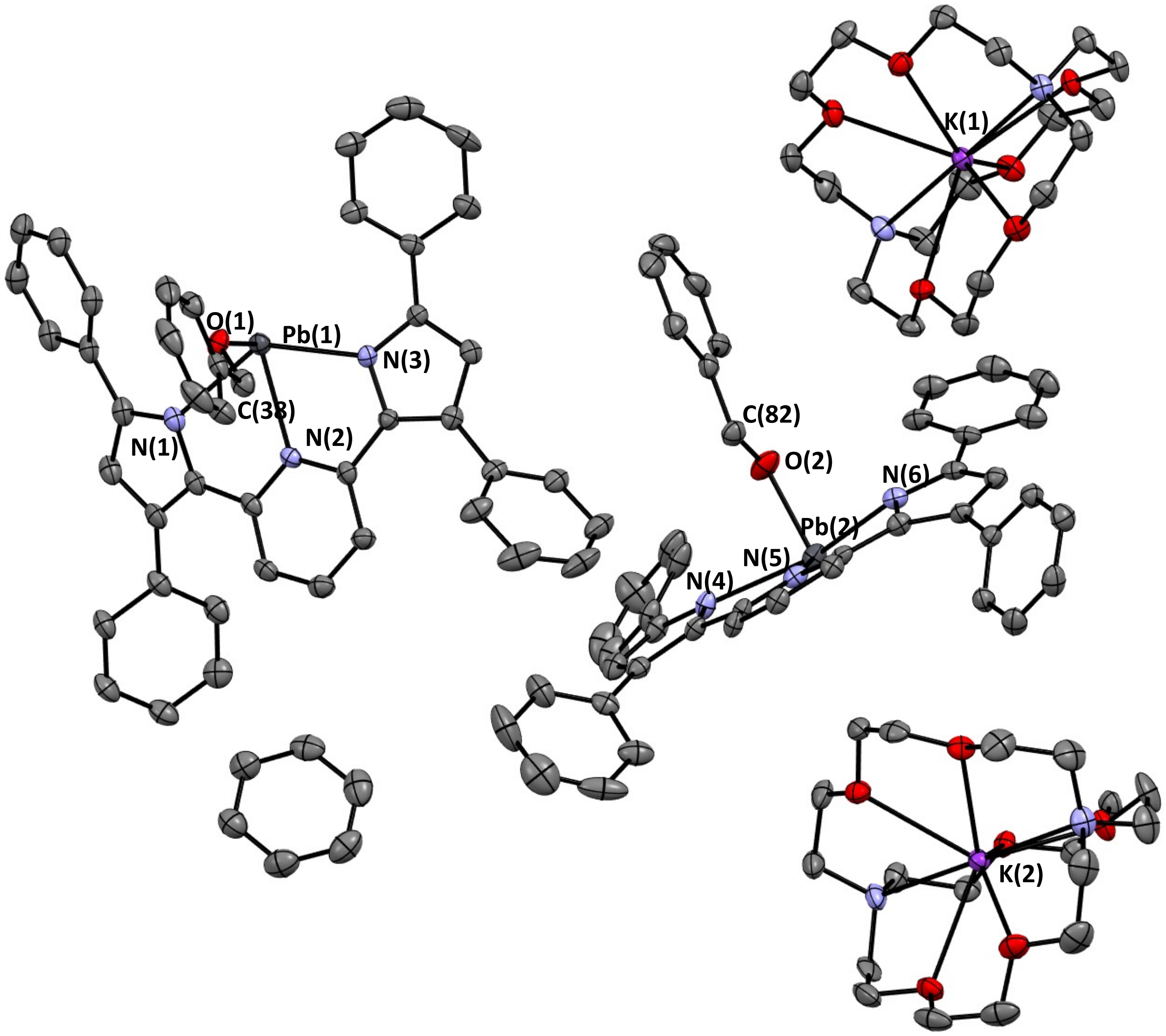

Figure S27. ORTEP diagram of **[Kcrypt222][1-OBz]** (30% thermal ellipsoids; hydrogen atoms omitted for clarity). Selected interatomic distances (Å) and angles (º): N(1)–Pb(1) 2.515(4), N(2)–Pb(1) 2.413(4), N(3)–Pb(1) 2.433(3), O(1)–Pb(1) 2.157(3), O(1)–C(38) 1.378(6), N(4)–Pb(2) 2.463(4), N(5)–Pb(2) 2.415(4), N(6)–Pb(2) 2.501(4), O(2)–Pb(2) 2.148(4), O(2)–C(82) 1.369(6); O(1)–Pb(1)–N(2) 92.43(12), C(38)–O(1)–Pb(1) 120.5(3), O(1)–Pb(1)–N(2) 101.29(13), C(82)–O(2)–Pb(2) 122.9(3).

4.Computational details

Density Functional Theory (DFT) calculations were performed with the Gaussian 16 suite of programs.[4] Geometry optimizations were applied by the means of the PBE0[5] hybrid functional, corrected for dispersion as proposed by Grimme (D3 correction, BJ damping),[6,7] and performed without any symmetry constraints using 6-311G(d,p) basis set for H, C, and N, and Def2-TZVP[8] basis set for Pb. NBO analyses were performed with NBO 6.0.[9] Input structures were taken from the experimentally observed X-ray diffraction structures of the anion **[1-H]** part of **[Kcrypt222][1-H]**.

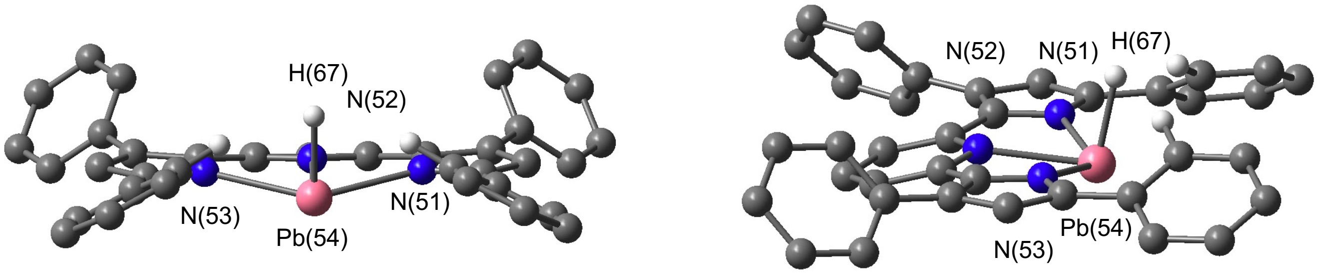

Figure S28. Optimized of molecular structure of **[1-H]**⁻ anion. Hydrogen atoms have been omitted for clarity. Selected interatomic distances (Å) and angles (º): N(51)–Pb(54) 2.493, N(52)–Pb(54) 2.431, N(53)–Pb(54) 2.493, H(67)–Pb(54) 1.866; N(51)–Pb(54)–N(52) 67.30, N(52)–Pb(54)–N(53) 67.30, N(51)–Pb(54)–N(53) 133.02, N(52)–Pb(54)–H(67) 95.8.

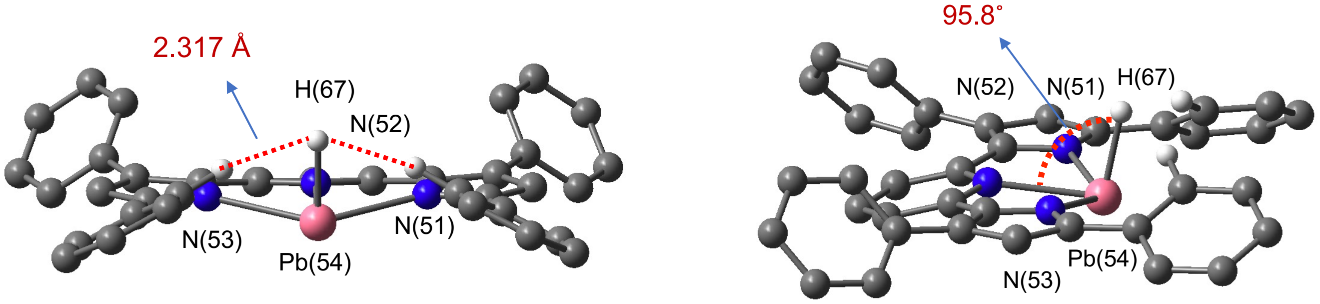

Figure S29 Selected interatomic distances showing DHB interactions (Å): H(67)–H(65) 2.317, H(67)–H(4) 2.317; and ∠H–Pb–N angle of 95.8º.

Table S4. Comparison of selected bond lengths and bond angles between solid state structure of **[Kcrypt222][1-H]**and calculated structure of **[1–H]**⁻

	Experimental (crystal structure) data of **[Kcrypt222][1-H]**	Calculated structure of **[1-H]**⁻
$N_{pyrrole}$–Pb	2.480(6) Å	2.493 Å
$N_{pyridine}$–Pb	2.397(6) Å	2.431 Å
$N_{pyrrole}$–Pb	2.474(6) Å	2.493 Å
Pb(54)–H(67)		1.866 Å
$N_{pyridine}$(52)–Pb(54)–H(67)		95.81°

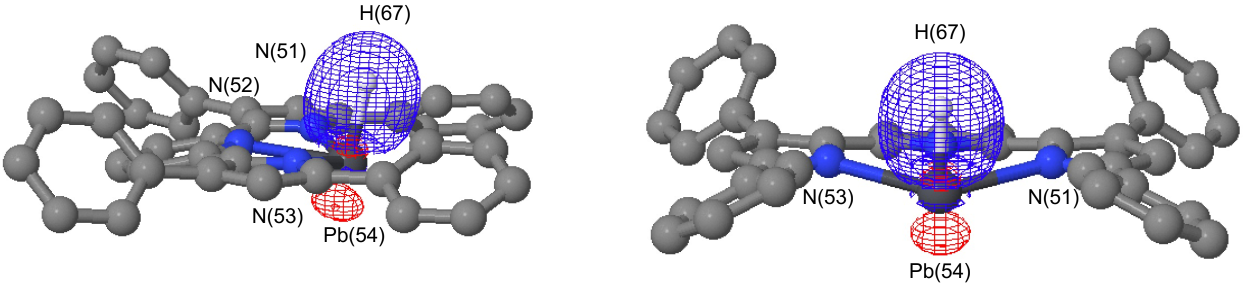

Figure S30 NBO diagram of **[1-H]**$^{-}$.

Coordinates for the optimized structure of **[1-H]**$^{-}$

C	3.54081300	-0.95363200	0.05399100
C	3.81309300	-2.38320300	0.14103300
C	2.90734700	-3.26350000	0.75021600
H	2.00603000	-2.86171200	1.20399300
C	3.17270300	-4.62420000	0.82089700
H	2.45284200	-5.28274400	1.29823500
C	4.35445000	-5.14308600	0.30212300
H	4.56050800	-6.20741800	0.35932500
C	5.27042000	-4.27838700	-0.29053800
H	6.19653900	-4.66860100	-0.70331200
C	5.00223000	-2.92023800	-0.37374800
H	5.70809000	-2.25723300	-0.86434700
C	4.47623400	0.08927500	0.02289700
H	5.55041200	-0.00122900	0.11787100
C	3.75344100	1.28943300	0.00259700
C	4.37969100	2.61089300	0.10444100
C	3.96125200	3.55435400	1.05343200
H	3.12919900	3.30366100	1.70339200
C	4.59420300	4.78343000	1.17093600
H	4.24810300	5.49536400	1.91458200
C	5.67463800	5.10089800	0.35274700
H	6.17113600	6.06171400	0.44698600
C	6.11174600	4.17146500	-0.58421800
H	6.95287600	4.40582400	-1.23044400
C	5.47093600	2.94509400	-0.70775000
H	5.80179000	2.22650400	-1.45105900
C	2.38697700	0.90513200	-0.01607100
C	1.17937500	1.68886900	-0.19955200
C	1.20059300	3.04795500	-0.53905600
H	2.14381300	3.55229300	-0.69025700
C	-0.00003800	3.71210600	-0.71547600
H	-0.00004700	4.75835500	-1.00759300
C	-1.20065800	3.04795400	-0.53899500
H	-2.14389300	3.55228800	-0.69013000
C	-1.17941000	1.68886500	-0.19951600
C	-2.38699900	0.90513100	-0.01600100
C	-3.75345500	1.28943800	0.00258000
C	-4.37967000	2.61093300	0.10418900
C	-3.96108700	3.55460000	1.05291100
H	-3.12896900	3.30402700	1.70283400
C	-4.59397500	4.78373000	1.17019000
H	-4.24776800	5.49582500	1.91363200
C	-5.67447700	5.10105100	0.35203300
H	-6.17092400	6.06191100	0.44609600
C	-6.11171000	4.17142500	-0.58468200

H	-6.95288500	4.40567300	-1.23088700
C	-5.47096100	2.94499900	-0.70799300
H	-5.80190700	2.22625400	-1.45111200
C	-4.47625400	0.08928700	0.02311000
H	-5.55042800	-0.00119800	0.11813200
N	2.28671500	-0.44745500	0.03317800
N	-0.00001400	1.03859200	-0.07538500
N	-2.28673500	-0.44745100	0.03333000
Pb	-0.00002400	-1.38140800	-0.30669700
C	-3.81311000	-2.38318600	0.14142500
C	-5.00228200	-2.92026500	-0.37323100
H	-5.70817400	-2.25730200	-0.86384300
C	-5.27046800	-4.27840600	-0.28988600
H	-6.19661500	-4.66865500	-0.70256600
C	-4.35446200	-5.14305400	0.30279200
H	-4.56051700	-6.20738100	0.36010000
C	-3.17268000	-4.62412400	0.82144300
H	-2.45278900	-5.28262800	1.29879300
C	-2.90732600	-3.26343100	0.75062600
H	-2.00597900	-2.86160500	1.20430900
C	-3.54083300	-0.95362400	0.05424000
H	0.00004500	-1.74622300	1.52374500

5.References

1 Nagata, T. & Tanaka, K. Syntheses of a 6-(2-Pyrrolyl)-2,2′ -bipyridine Derivative and Its Ruthenium Complex. *Bull. Chem. Soc. Jpn.* **75**, 2469-2470, (2002).

2 Glock, C. *et al.* Calcium, Strontium, Germanium, Tin, and Lead bis(trimethylsilyl)amido Derivatives and 2,2,6,6-Tetramethylpiperidido and N-isopropylphenylamido Derivatives of Potassium and Calcium. *Inorg. Synth.*, 15-31, (2018).

3 Espinal-Viguri, M., Neale, S. E., Coles, N. T., Macgregor, S. A. & Webster, R. L. Room Temperature Iron-Catalyzed Transfer Hydrogenation and Regioselective Deuteration of Carbon–Carbon Double Bonds. *J. Am. Chem. Soc.* **141**, 572-582, (2019).

4 Gaussian 16 Rev. C.01 (Wallingford, CT, 2016).

5 Adamo, C. & Barone, V. Toward reliable density functional methods without adjustable parameters: The PBE0 model. *J. Chem. Phys.* **110**, 6158-6170, (1999).

6 Grimme, S., Antony, J., Ehrlich, S. & Krieg, H. A consistent and accurate ab initio parametrization of density functional dispersion correction (DFT-D) for the 94 elements H-Pu. *J. Chem. Phys.* **132**, 154104, (2010).

7 Grimme, S., Ehrlich, S. & Goerigk, L. Effect of the damping function in dispersion corrected density functional theory. *J. Comput. Chem.* **32**, 1456-1465, (2011).

8 Weigend, F. & Ahlrichs, R. Balanced basis sets of split valence, triple zeta valence and quadruple zeta valence quality for H to Rn: Design and assessment of accuracy. *Phys. Chem. Chem. Phys.* **7**, 3297-3305, (2005).

9 Glendening, E. D., Landis, C. R. & Weinhold, F. NBO 6.0: Natural bond orbital analysis program. *J. Comput. Chem.* **34**, 1429-1437, (2013).